UNIVERSITA' DEGLI STUDI DI PARMA

Dottorato di ricerca in Fisiopatologia Sistemica

Ciclo XXIV

Morphological, ultrastructural and immunohistochemical identification of cardiac lymphatic vessels and their functional role in cardiomyopathies

Coordinatore:
Chiar.mo Prof. Enrico Maria Silini

Tutor:
Chiar.mo Prof. Federico Quaini

Dottorando: Dott. Stefano Cavalli

RIASSUNTO

Il sistema linfatico consiste in una fitta rete di capillari e vasi che vanno a formare un circolo aperto e monodirezionale parallelo a quello sanguigno. Tra le sue più importanti funzioni figurano l'assorbimento degli acidi grassi ed il mantenimento dell'omeostasi tissutale mediante drenaggio di liquidi e proteine plasmatiche fuoriuscite dai capillari sanguigni nei tessuti. Il circolo linfatico, attraverso le stazioni linfonodali, svolge anche un ruolo determinante nel trasporto delle cellule immunitarie, garantendo la sorveglianza immunologica e permettendo alle cellule immunitarie di raggiungere velocemente il sito di danno. Lo studio della circolazione linfatica è sempre più importante in oncologia, visto il suo coinvolgimento nei meccanismi di migrazione delle cellule neoplastiche che portano allo sviluppo di metastasi.

Lo studio dei vasi linfatici è stato per lungo tempo ostacolato dalla difficoltà nella loro identificazione e distinzione dai vasi sanguigni. La recente scoperta di marcatori come Podoplanina (PDPN), "lymphatic vessel endothelial hyaluronan receptor 1" (Lyve-1) e "Prospero- related homeobox 1"(Prox-1), che sono espressi specificamente in cellule endoteliali linfatiche, ha notevolmente favorito il loro studio istologico in tutti i distretti dell'organismo, compreso il cuore. Infatti, anche se la prima descrizione dei vasi linfatici nel cuore risale a circa tre secoli fa, solo di recente è stato rivalutato il loro ruolo sia nel mantenimento dell'omeostasi del tessuto interstiziale che in condizioni patologiche. Restano ancora da chiarire i meccanismi che regolano la linfangiogenesi a livello cardiaco ed i fattori di crescita coinvolti.

Il più rilevante sistema di regolazione della linfangiogenesi si sviluppa sull'asse VEGF-C/VEGFR-3, ma anche altri fattori di crescita si sono dimostrati capaci di stimolare la

crescita di vasi linfatici. Ad esempio il "Plateled derived growth factor" (PDGF) è un fattore di crescita da tempo conosciuto per la sua azione pro-angiogenica e il suo coinvolgimento nei meccanismi di reclutamento di cellule vascolari murali come i periciti. Recentemente è stata provata la sua importanza anche nell'induzione della linfangiogenesi tumorale.

La prima fase di questo lavoro consiste nella caratterizzazione immunofenotipica, strutturale ed ultrastrutturale dei vasi linfatici in diversi organi umani e murini. Sezioni istologiche, ottenute sia da campioni autoptici umani che da organi isolati da modelli sperimentali, sono state analizzate tramite tecnica immunoistochimica in fluorescenza per verificare l'espressione dei più importanti markers linfatici. I markers risultati più specifici e maggiormente espressi sono quindi stati selezionati per valutare fenotipo, densità e distribuzione del sistema linfatico.

La distribuzione dei vasi linfatici nel cuore umano e murino risulta simile. Questi si concentrano principalmente nelle regioni subepicardiche e negli spazi interstiziali che circondano arterie e vene. Un piccolo numero di capillari linfatici si ritrova nelle parti più profonde del muscolo cardiaco tra i cardiomiociti.

La successiva analisi mediante microscopia elettronica ci ha permesso di analizzare le caratteristiche ultrastrutturali associate ai vasi linfatici, non facilmente rilevabili con altre metodiche. I vasi linfatici mostrano una parete molto sottile rispetto ai vasi sanguigni, una membrana basale assente o discontinua e frequenti interruzioni del monostrato endoteliale, conosciute come fenestrature. Un'ulteriore conferma della natura linfatica dei vasi analizzati è stata ottenuta tramite tecnica Immunogold con anticorpi specifici per il Lyve-1.

Le tecniche precedentemente descritte ci hanno permesso di ottenere informazioni

esclusivamente bidimensionali, mentre l'architettura vascolare all'interno dell'organo è tridimensionale. Per superare questo limite tecnico è stato quindi messa a punto una nuova tecnica, denominata micro-linfangiografia in fluorescenza. In seguito all'iniezione di due traccianti fluorescenti, l'intero spessore del ventricolo di ratto viene analizzato al microscopio confocale. La tecnica permette di ottenere ricostruzioni tridimensionali della rete di vasi linfatici all'interno dell'organo.

Nella fase successiva del lavoro sono stati valutati gli aspetti funzionali del sistema linfatico cardiaco. Il tessuto cardiaco è stato analizzato sia nelle condizioni normali, sia nelle condizioni conseguenti allo sviluppo di diverse cardiomiopatie. Ognuna delle cardiomiopatie analizzate è scatenata da un diverso agente eziologico.

Nella cardiomiopatia ipertrofica ostruttiva (HOCM) è la mutazione di geni codificanti per proteine sarcomeriche a determinare lo sviluppo di ipertrofia settale accompagnata da disfunzione diastolica. Il danno ischemico è invece la causa scatenante della più comune cardiomiopatia di origine estrinseca, ovvero l'infarto del miocardio (MI). La cardiotossicità risulta infine tra i principali effetti avversi conseguenti al trattamento con diversi farmaci antitumorali come Doxorubicina e Imatinib . Il primo farmaco fa parte della famiglia delle antracicline, e come tale determina un effetto cardiotossico ampiamenente studiato e conosciuto. L'Imatinib è invece un inibitore dei recettori tirosina-chinasici (TKI) e rappresenta uno dei più grandi successi della medicina per quel che riguarda la cura delle neoplasie, approvato per il trattamento della leucemia mieloide cronica e dei tumori gastrointestinali. Tra i principali target dell'IM figurano recettori di grande importanza per la regolazione dell'angiogenesi nonché della linfangiogenesi, come il c-kit, il PDGFR e il VEGFR-3.

Lo studio di campioni derivanti da miectomie chirurgiche di pazienti affetti da HCM ha

messo in evidenza una forte risposta linfangiogenica all'interno dell'organo. I risultati dell'analisi immunoistochimica indicano una sensibile riduzione del numero di capillari sanguigni, in termini di densità (numero di vasi per unità di area analizzata). Questa alterazione del letto vascolare sanguigno risulta semplice da giustificare se si tiene conto di quelle che sono le principali caratteristiche istomorfologiche della malattia, ovvero la fibrosi interstiziale, l'aumento della dimensione dei miociti ed il loro disarray. Il comportamento del sistema linfatico ha però un andamento completamente diverso. Si osserva un aumento marcato della densità dei vasi linfatici sia a livello dello spesso strato di tessuto fibrotico presente nel versante subendocardico, sia a livello dei tessuti muscolari cardiaci più profondi. L'aumento in termini di densità è accompagnato da un altrettanto marcato incremento dell'indice proliferativo che è stato misurato andando a quantificare i livelli di espressione nucleare di proteine specifiche del ciclo cellulare e della mitosi.

Nella risposta dell'organo ad un insulto ischemico come l'infarto, è stato osservato un significativo aumento del numero dei vasi linfatici. Questo aumento risulta differito rispetto alla risposta angiogenica e funzionalmente associato alle diverse fasi di maturazione della cicatrice fibrotica.

Anche nella cardiotossicità indotta da DOXO si registra un aumento di densità della componente linfatica associata alla marcata deposizione di collagene tipica di questa cardiopatia.

Un comportamento completamente diverso si osserva invece nella cardiotossicità indotta da IM. Il cuore degli animali trattati con il farmaco mostra, in associazione ad una forte riduzione dei vasi linfatici, un aumento nel contenuto relativo di acqua. Il trattamento con il farmaco è quindi in grado di alterare la funzione di drenaggio del

miocardio contribuendo allo sviluppo della disfunzione dell'organo. A livello ultrastrutturale, abbiamo inoltre potuto documentare in microscopia elettronica un'estesa compromissione dei mitocondri nei vasi sanguigni e linfatici.

In conclusione i dati ottenuti dimostrano che, in ognuna delle condizioni patologiche analizzate, il sistema linfatico risulta importante nella risposta del cuore ai diversi insulti subiti ed assume un ruolo determinante per il suo rimodellamento. L'interferenza nei meccanismi linfangiogenici può determinare un'alterazione dell'omeostasi tissutale e quindi contribuire negativamente allo sviluppo di cardiopatie

INTRODUCTION

THE LYMPHATIC VASCULATURE

The lymphatic system comprises a one way, open-ended complex network of capillaries, precollecting and collecting trunks, ducts and lymph nodes. It is involved in transport of tissue fluids, extravasated plasma proteins and cells back into the blood circulation. Lymph is formed when interstitial fluids enter the terminal lymphatic capillaries that drain the lymph to larger contractile lymphatics, which possess valves as well as a smooth muscle wall and are called the collecting lymphatics[1]**.** As the collecting lymph vessel accumulates lymph from more and more capillaries in its course, it becomes larger and represents the afferent lymph vessel as it enters a lymph node. Here the lymph percolates through the lymph node tissue and is removed by the efferent lymph vessel. An efferent lymph vessel may directly drain into one of the large lymph ducts (right or thoracic), or may empty into another lymph node as its afferent lymph vessel[2]**.** Both lymph ducts return the lymph to the blood stream by emptying into the subclavian veins[3].

In spite of these connections and the close juxtaposition of lymphatic vessels with vein and arteries, this system is anatomically and entirely separated from the blood circulatory system. Anatomically, lymphatic vessels differ from blood ones in several ways. The lymphatic capillaries are made up of a single-cell layer of endothelial cells that form a thin-walled, fenestrated and blinded vessel lacking pericytes and a continuous basal lamina.

The presence of specific junctional proteins between endothelial cells of initial lymphatics has been recently described. The endothelium of initial lymphatics contains vascular endothelial cadherin (VE-cadherin) and platelet endothelial cell adhesion molecule-1 (PECAM-1). These proteins are typical of both adherens junctions and tight

junctions and are partially colocalized at the borders of oak leaf-shaped endothelial cells to form discontinuous, button-like junctions (buttons) structurally different from the zipper-like junctions (zippers). Regions between buttons in initial lymphatics are openings where fluid can enter without repetitive formation and dissolution of intercellular junctions[4].

Lymphatic capillaries also possess anchoring filaments, specialized extracellular fibrillar structures linking lymphatic endothelial cells (LECs) to the extracellular matrix, which also help to maintain the patency of the vessels in conditions of high interstitial pressure or inflammatory state, facilitating the uptake of fluid, macromolecules and cells[5,6,7]. The lymphatic system, unlike the blood lacks a central pump. The force driving the lymph is generated by the contraction of smooth muscle cells laying on the collecting vessels, by respiratory movements and by squeezing of skeletal muscle contraction[8]. Lymphatic pre-collecting and collecting trunks have a different structure than lymphatic capillaries: in addition to their large diameter they are surrounded by a muscular wall and by the presence of internal valves prevent the retrograde flow of lymph fluid.

The main role of the lymphatic vascular system is the maintenance of tissue fluid pressure homeostasis by draining excess interstitial fluid leaking from blood capillaries. Furthermore, the lymphatic system plays a central role in the immune reactions allowing the circulation of immune cells to and from the lymph nodes. Lymphatic system for example is the migration way of antigen-presenting cells (APCs), such as dendritic cells, from tissues to lymph nodes in immune surveillance. Recently ymphatics have gained relevance in oncology because they are also routes for spreading cancer cells [9,10,11]. The lymphatic system may be also implicated in drainage and

clearance of toxic substances from tissues. Finally, the lymphatic vessels in the intestine is involved in the dietary fat (lipids and fat-soluble vitamins A, E, D and K) absorption and subsequent transport to the circulatory system.

Although the function and structure of lymphatic vessels are partially defined, its embryonic development is still partially known. Two alternative mechanisms have been proposed to explain the origin of the lymphatic system. The most widely accepted view was proposed by Florence Sabin in the 1902, indicating that lymphatic vessels originate from a primitive lymph sacs generated by endothelial cells, which sprout from the cardinal vein during the early stages of development. Lymphatic vessels grow out "centrifugally" from these sacs[12]. In contrast, an alternative model proposes an autonomous origin of the lymphatic system from mesenchymal precursor cells. By this hypothesis, lymphatic vessels evolve independently from the embryonic vein and the connections between two vascular systems are established during a later phase of development[13].

The investigation of lymphatic vessels has been long hampered by the difficulty in their identification and distinction from blood vessels, particularly from venules. Moreover, when lymphatics are not filled with lymph, they tend to collapse and may become impossible to recognize. The recent discovery of several lymphatic endothelial cell-specific markers that consistently and specifically reacts with lymphatic endothelium, has made histological study of lymphatic vessels feasible. The first marker expressed in the initial stage of lymphatic development is "lymphatic vessel endothelial hyaluronan receptor 1"(Lyve-1)[14]. This marker is an integral membrane glycoprotein, homolog of the hyaluronan receptor CD44[15]. Lyve-1 is expressed in a subpopulation of endothelial cells localized in the cardinal vein in the early stage of lymphatic

development. In adults, the expression of Lyve-1 is extended to liver sinusoids, some lung blood vessels, high endothelial venules and active tissue macrophages[16]. However, Lyve-1 does not seem to be essential for the lymphatic system since transgenic mice lacking this protein exhibit a normal development of lymphatic vessels and immune cell trafficking[17].

Among the complex network regulated by Vascular Endothelial Growth Factors (VEGFs), the receptor 3 (VEGFR-3), is specific for lymphangiogenic factors VEGF-C and VEGF-D[18,19]. During the early stage of development, this receptor is highly expressed in the blood vascular endothelial cells, but after mid-gestation it is expressed only by lymphatic endothelial cells. Genetic manipulation of VEGFR-3 affects lymphatic development. All VEGFR-3 knock-out mice die in utero of cardiac failure before lymphatic vessels formation[20,21]. The expression of this receptor is a key element involved in the establishment of LECs identity and is tightly related to another important lymphatic marker: the "Prospero- related homeobox 1"(Prox-1). Prox-1 is a transcription factor strictly required for the specification of LECs since it is expressed during all stage of development only in lymphatic vessels[22,23]. Prox1 is initially expressed by a subpopulation of cells in the cardinal vein[24]. Its activation induces the expression of LECs-specific genes like Podoplanin and VEGFR-3 and downregulates genes involved in blood endothelial cells (BECs) specification[25]. Lyve-1^{pos}/Prox-1^{pos} cells are able to bud off from cardinal vein in a polarized manner. Subsequently, these budding LEC progenitors proliferate and migrate to form the embryonic lymph sac and lymphatic vascular network. Total or partial inactivation of Prox1 result in a lymphatic hypoplasia and a general failure in LECs differentiation with a complete lack of lymphatic vasculature in the absence of defects of the blood stream[22]. Moreover, the

temporal inactivation of Prox1 alters the phenotypic commitment into mature LECs and reverts them to BECs identity[26]. These data prove the importance of prox-1 expression for LECs specification and maintenance, not only during the embryonic development but also in the adult life. After the formation of lymph sacs, the Lyve-1^{pos}/Prox-1^{pos} cells begin to form a capillary network.

In this stage cells express another marker, the mucin-type transmenbrane glycoprotein, Podoplanin (Pdpn). Pdpn null mice die at birth due to respiratory failure and have defects in lymphatic but not in blood vessel pattern formation. These defects are associated with diminished lymph transport, congenital lymphoedema and dilation of lymphatic vessels[27,28]. Pdpn may contribute to LECs adhesion and migration, and may induce proper connections between superficial and deep lymphatic plexuses.

Tab 1: Markers of lymphatic (LEC) and blood vascular endothelial (BEC) cells

Marker	Molecular function	LEC	BEC	References
PROX-1	Transcription factor	++	-	21
Pdpn	Transmembrane glycoprotein	++	-	24
CD31	Adhesion molecule	+	++	Albeda[29]
CD34	Adhesion molecule	- (+)[a]	++	Young[30]
CD44	Hyaluronan receptor	-	+	Kriehuber[31]
LYVE-1	Hyaluronan receptor	++	-	12, 13
VEGFR-3	Tyrosine kinase receptor	++	- (+)[b]	17

[a] CD34 expression has been also detected on LECs
[b] VEGFR-3 expression has been observed in tumor-associated blood vessels

THE CARDIAC LYMPHATIC SYSTEM

Although the description of the presence of lymphatics in the heart has been reported over three century ago, their role and function in normal and pathologic states are still largely unclear due to the intrinsic technical difficulty to study the cardiac lymph flow and lymphatic vessels. The recent identification of lymphatic endothelial cell-specific markers, the generation of new animal models and lymphatic vascular imaging technology led to a reevaluation of the importance of cardiac lymphatic vasculature in the control of heart function. The principal role of the cardiac lymphatic system appears to be restricted to the maintenance of tissue fluid homeostasis, although an active role also in immune responses to inflammatory state and in cardiac failure has recently emerged. A series of observations allowed to correlate the interruption of the lymphatic flow with significant anatomic and functional changes of the heart[32,33]. The first technique to identify cardiac lymphatics utilized the injection of a dye[34]. Initial studies based on this technique were able to identify and describe the lymphatic system organization in the heart. Cardiac lymphatic vessels have been found in several aspects of the cardiac wall including the subepicardium, mid-myocardium and subendocardium[35,36]. The principal limitation of this technique is that only "non contracting" lymphatic vessels are detectable whereas collapsed vessels cannot be filled by the dye[37].

In the mammalian heart, two forms of cardiac lymphatic vasculature have been described: the lymphatic capillary plexus and the collecting lymphatic vessels. The lymphatic capillary plexus is present in the mid-myocardium and subendocardium where it lies parallel to the endocardial surface. The collecting lymphatic vessels can be seen in the subepicardium where they join into single or multiple collecting trunks.

These structures proceed toward mediastinal lymphatic vessels and then merge into subclavian vein, completing the lymph flow circuit. The cardiac lymph flow is controlled by active and passive lymphatic pumping. The active part is generated by spontaneous contraction of muscle cells of the collecting vessel wall but has a limited capacity to drain large quantity of fluid. In contrast, other forces related to cardiac muscle contraction that probably represents the major way of draining lymph fluid drive passive lymphatic flow[38,39].

A series of recent promising research studies have underlined the beneficial effect of active lymph drainage on heart function, especially in cardiac pathologies. Analyzing autoptic tissues of the human heart, Ishikawa et al. have tried to elucidate the role of the lymphatic system in the entire process of tissue repair and scar formation after myocardial infarction (MI)[40]. According to this study, lymphangiogenesis takes place after blood vessel angiogenesis and may be involved mainly in the maturation of fibrotic tissue and in the definition of scar formation through the drainage of excessive proteins and fluids. Specifically, lymphatic vessels are absent in the early stages of scar formation, in which blood capillaries prevail to decrease thereafter with the progression of the infarct. In parallel, lymphatic vessels begin to appear in the peripheral area near the infarct. Subsequently, they appear as dilated structures in the peripheral area and with capillary features in the central area of granulation tissue. Later in the completion of myocardial infarction, lymphatic density increases during the final stage of scar formation. These results demonstrate that active drainage of fluids and removal of the end products of cellular damage by lymphatics play an important role in the determination of tissue response to an acute ischemic insult.

PDGFR SIGNALING AND LYMPHANGIOGENESIS

PDGFRs are surface tyrosine kinase receptors for members of the platelet-derived growth factor (PDGF) family. These receptors are involved in many biological functions such as cell proliferation, differentiation, growth and tissue development. Autocrine activation of PDGFR signaling pathway is also implicated in a variety of diseases including cancer[41]. There are two forms of the PDGF-R, alpha and beta, each encoded by a different gene[42]. This receptor is expressed by perivascular mesenchymal cells, likely representing vascular mural cell progenitors (vSMC and pericytes). In particular, PDGFR beta (β) is strongly expressed in tip cells of the angiogenic sprouts and in the endotelium of growing arteries at sites where pericytes are actively recruited and vSMC population is expanding[43,44].

It should be emphasized that PDGF-B and PDGFR-β knock-out mice exhibit hemorrhagic and edematous phenotypes in early embryos due to defective development and recruitment of vascular mural cells (pericytes and SMC) onto blood vessels. PDGF receptors have been localized on blood vessel endothelial cells, suggesting a direct role of PDGFs on angiogenesis[45]. However, recent studies suggest that members of the PDGF family including PDGF-AA, -AB and -BB are able to induce lymphatic vessel growth in the mouse cornea[46]. The mechanism of this PDGF induced lymphangiogenesis is not still clear, although an indirect participation of the VEGF-C/-D/VEGFR-3 signaling pathway has been proposed. Thus, PDGF combined with their receptors constitute a very important system regulating both angiogenesis and lymphangiogenesis.

HYPERTROPHIC OBSTRUCTIVE CARDIOMYOPATHY

Hypertrophic cardiomyophathy (HCM) is a primary cardiac disorder characterized by asymmetrical hypertrophy of the left ventricle in the absence of conditions that could lead to an hemodynamic overload (aortic stenosis, hypertension, thyroid disease).[47]

Since its initial description in 1958, this pathology has generated intense investigation.[48,49,50,51,52] HCM is a congenital cardiac disorder inherited as an autosomal dominant trait and its genetic basis are well defined. Most of the genes involved, encode for proteins linked to the contractile unit of the cardiomyocyte.[53,54,55,56,57]

The complexity of this disorder is remarkable by a heterogeneous clinical presentations, ranging from no symptoms to severe heart failure and sudden cardiac death.[58]

To date, the molecular steps linking the genetic mutation to the clinical phenotype remain still undiscovered.

About 30-50% of individuals with HCM demonstrate an obstruction to the left ventricular outflow caused by asymmetric septal hypertrophy.

The obstructive variant of HCM, Hypertrophic obstructive cardiomyopathy (HOCM) is also historically known as idiopathic hypertrophic subaortic stenosis (IHSS) and asymmetric septal hypertrophy (ASH).

Surgical septal myectomy is reserved for those patients who, despite drug therapy, still show severe symptoms with a marked obstruction of the septum and an unacceptable lifestyle.[59]

ANTICANCER DRUG CARDIOTOXICITY

Several chemotherapeutic drugs have been implicated in cardiotoxicity. In particular, anthracyclines have been clearly identified as a cardiotoxic agent, however also Tyrosine Kinase Inhibitors (TKIs)[60] have been shown to induce cardiovascular events.

Anthracyclines are one of the most active anti-neoplastic drugs against hematologic[61] and solid[62] tumors, however, their cardiotoxic adverse effects such as cardiomyopathy and symptomatic Congestive Heart Failure (CHF) have limited their clinical use. Doxorubicin (DOXO) is a member of anthracyclines family. The mechanism of action of DOXO is complex and still somewhat unclear, although is known that DOXO interact with DNA by intercalation and inhibition of macromolecular biosyntesis. In particular, DOXO stabilizes topoisomerase II complex after its breaking action on the DNA chain for replication. This event prevents the DNA double helix from being resealed and thereby stopping the process of replication. Like other chemotherapeutic agents, DOXO do not possess a specific activity on cancer cells, but also affects normal cells, leading to severe side effect. Moreover, anthracyclines are known for causing cardiotoxicity that most often manifests many years after treatment. Cardiotoxicity may be due to different deleterious events in cardiac muscle cells, which include interference with the ryanodine receptors of the sarcoplasmic reticulum, free radical formation or severe metabolic dearrangement.

TKIs represent a decisive turning point in the modern medicine, since they specifically interfere with the proliferation/apoptosis pathways of neoplastic cells, and their introduction gained a formidable increase in survival rates of patients affected by specific cancer. Tyrosine kinases play a critical role in the modulation of growth factor

signaling. Activated forms of these enzymes can cause increases in tumor cell proliferation and growth, induce anti-apoptotic effects, and promote angiogenesis and metastasis. Because all these effects are initiated by receptor tyrosine kinase activation (also caused by somatic mutation), these enzymes are key targets for inhibitors. TKIs are examples of the recent trend toward targeting multiple receptor kinases, such as Vascular Endothelial Growth Factor (VEGF) receptor 1–3, Platelets Derived Growth Factor (PDGF) receptor α/β, KIT, FMS-related tyrosine kinase 3 (FLT3), colony-stimulating factor 1 receptor (CSF1R) and rearranged during transfection (RET) receptor tyrosine kinases.[63] Although this class of drugs directly aims oncogenic pathways, the clinical use of TKIs resulted in alteration of cardiac function. Although TKIs toxic effect seems to be manageable and reversible at a short- or mid- term follow-up, the development of late cardiovascular sequelae is more than a speculative possibility. Unfortunately, differences between pediatric, adult, and elderly patients and the lack of uniform modality in detecting and reporting cardiac events makes adequate estimates even more difficult[64,65]. Thus, it seems to be necessary to deepen our understanding on the mechanisms of cardiotoxicity, whose explanation have been so far ambiguous.

AIM

The aim of our study was to characterize the cardiac lymphatic system and to evaluate its role in four different pathological conditions .

To obtain background information, our ability to detect lymphatic vessels was extensively challenged by studying human and animal tissues with immunofluorescence and confocal microscopy. Moreover, fluorescence micro-lymphangiography on whole mount preparations of the heart and skin from rats were employed to define by confocal microscopy the lymphatic architecture and 3D reconstruction. Additional studies were performed to characterize ultrastructural aspects of lymphatics by Transmission Electron Microscopy (TEM) implemented by immunogold labelling.

The first pathological study was performed in a mouse model of myocardial infarction (MI), to ascertain the role of lymphangiogenesis in the entire process of myocardial repair and scar formation.

Then we tested lymphatics behavior in hypertrophic obstructive cardiomyopathy (HOCM), a genetically defined cardiomyopathy also resulting, through different mechanisms, in collagen deposition and fibrotic scarring.

Subsequently, we focused our attention on Imatinib Mesylate (IM) (Gleevec©, Novartis, Basel, Switzerland) a small-molecule TKIs, whose introduction revolutionized the treatment and the survival rate of Chronic Myeloid Leukemia (CML) and other types of tumors[66,67]. Our interest has been specifically addressed to IM because it possesses a potent activity against c-KIT and PDGFR, tyrosine kinase receptors involved in lymphangiogenesis and closely related to the phenotype of Cardiac Progenitor Cells (CPCs). In a rat model of IM induced cardiomyopathy we attempted to demonstrate that impairment of lymphangiogenesis may affect cardiac structure and

function.

Finally, to assess whether inhibition of lymphatics was a specific effect of TKI or a common mechanism implicated in cardiotoxicity, the analysis of lymphatic structures was conducted in a model of DOXO induced cardiomyopathy.

MATERIAL AND METHODS

Human tissue samples

Normal human myocardial and skin samples were collected from archive material of autopsies performed by the Department of Pathology, University of Parma. Only cases devoid of cardiovascular or cutaneous diseases were included in this study. Tissue specimens obtained within 24-48 hours after death, were embedded in paraffin and 5 μm histological sections were obtained for the immunohistochemical analysis of lymphatic vessels.

Lung tissue was collected from patients affected by lung cancer and undergoing lung resections, enrolled after informed consent to the employment of biologic samples for research purpose. Transported under sterile condition to the Department of Pathologic Anatomy, samples were dissected under hood at laminar flow.
Portions of healthy lung tissue were sampled by the medical staff ensuring the priority of their use for diagnostic purposes. The correct sampling procedure was confirmed by the subsequent histologic analysis.

Left ventricular myocardial fragments were obtained from 31 patients affected by HOCM undergoing septal myotomy-myectomy.

Hypertrophic heart specimens were obtained from patients with aortic stenosis (AoS) undergoing valve replacement for rheumatic disease or degenerative calcification. Myectomies collected were the waste material of outflow tract releasing surgical interventions.

All collected samples were formalin fixed and paraffin embedded for morphometric analysis and immunohistochemistry.

Experimental models

The study population consisted of male Wistar rats (*Rattus norvegicus,* IM model), Female Fischer 344 rats (DOXO model) and male CD1 mice (MI model) breed in our departmental animal facility. Animals were kept in unisexual groups of four individuals from weaning (4wk after birth) until the onset of the experiments, in a temperature-controlled room at 22–24 °C, with the light on between 7.00 AM and 7.00 PM. The bedding of the cages consisted of wood shavings, and food and water were freely available. The investigation was approved by the Veterinary Animal Care and Use Committee of the University of Parma and conformed with the National Ethical Guidelines (Italian Ministry of Health; D.L.vo 116, January 27, 1992) and the Guide for the Care and Use of Laboratory Animals (NIH publication no. 85–23, revised 1996).

Animal model of myocardial infarction (MI)

MI was induced in male CD1 mice weighing 35-40g (Charles River, Comerio, Italia) by permanent ligation of left anterior descending artery using a 6 to 0 silk suture. Sham-operated animals underwent a similar procedure without ligation.

Each animal was anaesthetized with a solution of Xilazine (2.5mg/Kg) and Ketamine (50mg/Kg.) and the surgery was performed with mechanical ventilation. (volume: 8-9 mL/g; frequency: 165/min). After autonomous respiratory recovery, animals were placed in the cage alone. Mortality observed after surgery was less than 10%.

Animal model of Doxorubicin induced cardiomyopathy

Female Fischer 344 rats (n=160) at 3 months of age (body weight 180±10 g) received DOXO in six equal intraperitoneal injections of 2.5 mg/kg b.w over a period of 2 weeks to reach a cumulative dose of 15 mg/kg b.w. .Control rats (CTRL) were injected with the vehicle alone (lactose, 75 mg/kg in saline) in the same regimen as DOXO. Animals were sacrificed at 3 weeks after the first injection.

DOXO solution was obtained by dissolution of powder (Pharmacia-Upjohn, Milan, Italy) in vehicle solution (1% lactose in sterile saline) at a concentration of 0.15 mg/ ml.

Animal model of IM induced cardiomyopathy

Thirty four 8 wk old rats, weighing 200 - 250 g were divided into three groups. (1) IM50 (n=8), animals subjected to intra-peritoneal (i.p.) injections of 50mg/kg IM three times a week for three weeks; (2) IM100 (n=10), animals subjected to i.p. injections of 100mg/kg IM three times a week for three weeks; (3) CTRL (n=8), animals injected with equal volume of saline and taken as control. Rats were anesthetized with droperidol + fentanyl citrate (Leptofen, Farmitalia-Carlo Erba, Milan, Italy; 1.5mg/kg im) which we have found to induce negligible changes in cardiovascular parameters when telemetrically recorded in conscious animals (unpublished data). Finally, hemodynamic data were invasively collected and the heart of each animal was perfusion fixed for morphometric and immunohistochemical studies.

IM 100 mg capsules were a gentle gift of the Department of Hemathology, representing discarded material from patient's drug withdrawal. The capsules were dissolved with prolonged stirring in sterile water previously adjusted at ph=2 with 10N HCl and then, before the injection, re-adjusted at pH=6,2 with sodium hydroxide

(NaOH) 10N. The suspension was finally filtered to obtain a sterile solution devoid of solid particles and stored in aliquots at -80 °C. At the time of administration the drug was diluted according to the desired concentration and to a volume of injection ranging from a minimum of 0.7 to a maximum of 1.2 ml.

Anatomical parameters

The hearts of anesthetized animals were arrested in diastole by injection of 5 ml cadmium chloride solution (100 mmol, iv) and the myocardial vasculature shortly perfused at a physiological pressure with a heparinized PBS-solution, followed by perfusion with 10% formalin solution. The heart was then excised and placed in formalin solution (10%) for 24 hours.

Then, the right ventricle (RV) and the left ventricle (LV) inclusive of the septum were separated. Subsequently, the heart was sliced in three 1-mm thick transversal sections, at the basal, equatorial and apical levels of the ventricle. Afterwards, the sections were embedded in paraffin. Five-µm thick slices were finally cut from the equatorial portion of the LV free wall for morphometric and immunohistochemical studies.

Theoretical water content

Hearts harvested from IM treated and control rats were cleaned from other tissues, major vessels and from excess water and blood. Subsequently, the entire atria and fragments of the septum, left and right ventricles were separately weighed. Thereafter, tissues were weighed after dehydration, achieved by several microwave heating cycles until non changes in weight of each individual tissue fragment was

measured. The wet weight to dry weight ratio was then computed and theoretical water content was obtained.

Immunohistochemical analysis

Five-micrometer-thick sections obtained both from human samples and from each group of animals were analyzed under fluorescence microscopy to determine the effects induced by the different cardiopathies on lymphatic and blood vessel density. Sections were incubated with lymphatic specific primary antibodies: polyclonal rabbit to LYVE1, (cod.ab14917, Abcam, Cambridge UK) Polyclonal rabbit to Prox1 (cod DP6501PX, Acris Herford Germany); monoclonal mouse to D2-40, (cod CM266, Biocare, Concord USA). For the identification of blood vessels, monoclonal mouse anti-α-smooth muscle actin antibody, (cod a5228, Sigma St. Louis, MO) and polyclonal rabbit anti-von Willebrand factor (vWF, cod F3520, Sigma St. Louis, MO) were used. Myocytes were identified by staining the same sections with monoclonal mouse anti-α-sarcomeric actin antibody (anti-α-SARC; cod.a2172, Sigma St. Louis, MO). Mitotic cells were recognized by the nuclear expression of the phosphorylated form of histone H3 (Ph-H3, cod.06-755, Millipore Corporation, Billerica, MA, USA,).

Tissue sections were incubated, respectively, with the primary antibodies followed by conjugated specific secondary antibodies.

FITC, TRITC-, Cy5- conjugated anti-mouse, anti-rabbit secondary antibodies (Jackson Laboratory, Baltimore, PA, USA) were used to detect simultaneously the different epitopes. Nuclei were recognized by DAPI (4',6-diamidine-2-phenyndole, Sigma St. Louis, MO) staining.

Ultrastructural and immunoelectron microscopic (ImmunoGold) detection of lymphatic vessels

Hearts harvested from normal and IM treated rats were analyzed by transmission electron microscopy (TEM) to detect structural and subcellular alterations involving lymphatic vasculature.

For ultrastructural analysis, the specimens of interest were fixed in 2.5% gluteraldehyde for 6 h. The tissues were then postfixed in 1% osmium tetroxide (OsO4) and dehydrated by increasing concentrations of alcohol. Following this procedure, samples were washed with propylene oxide and embedded in epoxy resin embedding media. Sections of 0.5 μm thickness were stained with methylene blue and safranin to select morphologically the field of interest. Subsequently, ultrathin sections were collected on a 300-mesh copper grid and, after staining with uranyl acetate and lead citrate, were qualitatively examined under a transmission electron microscope (Philips EM 208S).

For ImmunoGold detection the grids were incubated for 10 min in sodium periodate, a saturated solution necessary for the etching. After a series of washing the grids were incubated with Na-borohydride for 5 min and TBS pH 8 for 10 min; afterward sections were saturated with BSA 2% for 30 min an then incubated at 4°C overnight with the primary antibody polyclonal rabbit anti-LYVE1, (cod.ab14917, Abcam Cambridge, UK). Grids were rinsed for 3 × 5 min in TBS (ph 8) and BSA for 10 min and then incubated for 1 hr with goat anti-rabbit IgG conjugated with 10 nm gold particles (EMGAR10, BBI, United Kingdom) diluted 1:10 in TBS (pH 8.2). After rinsing for 2 × 5 min in TBS (pH 8.2) and distilled water (dH20), grids were contrasted with 4% uranyl acetate in 50% ethanol and lead citrate, for 20 and 10 min, respectively.

Negative controls consisted of samples in which the immunoreaction was performed in with the use of an indifferent primary antibody. Although the immunogold methodology has been utilized by our Pathology laboratory since at least 2 decades, its specificty was tested in our preparations by using an antibody highly expressed in the myocardium such as a-smooth muscle actin followed by goat anti-mouse IgG conjugated with 10 nm gold particles.

Fluorescence micro-lymphangiography

Lymphatic and blood vessel microvascular tridimensional architecture was studied by double-label whole-mount confocal microscopy.

Wistar Rats were anesthetized with droperidol + fentanyl citrate (Leptofen, Farmitalia-Carlo Erba, Milan, Italy; 1.5mg/kg im), and the jugular vein was catheterized by a PE50 polypropilen cannula. One ml of the fluorescent vascular tracer BSA-FITC (66 kDa; 30 mg/ rat, Sigma, St. Louis, MO) was injected intravenously. Rats were sacrificed 2 hours later, 3 minutes after 1 ml intravenous injection of a second fluorescent dye, Dextran-TRITC (160 kDa; 15 mg/rat, Sigma, St. Louis, MO), which served as a blood marker.

Time interval from first injection to sacrifice is enough to allow BSA-FITC leakage from vascular bed to interstitium and then to lymphatic vessels. Delayed injection of the second tracer otherwise impede the same route confining Dextran-TRITC into blood vessels. Thus, blood vessels are labeled with both dyes, whereas draining lymphatics are labeled only by the green fluorescence of FITC.

Samples of the skin and heart were removed and fixed overnight in 4% paraformaldehyde. To decrease light scattering during imaging, tissues were optically cleared as described below. Briefly, specimens were processed in 20-ml plastic vials

and using a tissue rotator. The tissue was first washed extensively in PBS to remove paraformaldehyde. Specimens were then dehydrated with successive 15-min washes through a graded methanol (MeOH) series (25%, 50%, 75%, 95% and 100% v/v in distilled water). Tissue was cleared using Murray's clear (BABB), a solution of 1 part benzyl alcohol to 2 benzyl benzoate (v/v) (both from Sigma-Aldrich, St. Louis, MO). Specimens were run through a series of 3:1, 1:1 and 1:3 (v/v) MeOH: BABB and left in 100% BABB for one week, until the tissue was transparent.

Specimens were examined using the Axiovert 200M inverted microscope (Carl Zeiss, Jena, Germany), integrated with the confocal system LSM 510 Meta scan head. Cleared whole-mount tissues mounted into a special Plexiglas chamber, were examined under 10× and 20× air objectives lenses. Images were scanned in fluorescence modes. Serial optical sections were recorded beginning at the top surface of the specimen, and the resultant stacks were rendered in three dimensions using AxioVision© (Carl Zeiss Imaging Solutions) and Huygens© (Scientific Volume Imaging) software to examine the 3D nature of the vascular network.

RESULTS

CHARACTERIZATION OF LYMPHATIC VASCULATURE IN NORMAL HUMAN TISSUES

Several normal fetal and adult human tissue samples were examined to evaluate the specific expression of lymphatic endothelial cell markers. Histological sections were collected from autopsies and analyzed by immunofluorescence.

Fetal and Adult Lung

In the fetal lung, Pdpn is not exclusively expressed by lymphatic vessels, but is also present in type I pneumocytes precursors. In agreement with this finding, terminal bronchiolar profiles resulted Pdpn positive (Fig 1A). We also observed that the number of lymphatic vessels change during lung development (data not shown). In the canalicular phase the tissue shows the highest amount of lymphatics to progressively decrease thereafter.

In adult lung a large amount of pulmonary Pdpn positive lymphatic vessels are located in association with bronchovascular bundles. Their presence within the lobule, the deeper part of the lung parenchyma, has been debated for years, particularly in regard to the presence or absence of true alveolar lymphatics[68697071]. Our study give a clear answer to this discussion, indeed we found small lymphatics also in interalveolar areas (Fig 1B). In addition, the connective tissue of the visceral pleura seem particularly rich in lymphatics. Quantitative overall estimation of the tissue indicates an average lymphatic density of $2,75 \pm 1,1/mm^2$.

In all lung developmental stages, from fetal to adulthood, lymphatic vessels are well distinguishable from blood vasculature, because the expression of Pdpn is not accompanied by the blood endothelial cell marker vWF (Fig 1A,B).

Fetal and Adult Heart

IHC analysis of fetal human hearts demonstrated that Pdpn is exclusively expressed by lymphatics and Pdpn negative blood vessels are positive for vWF.

Lymphatic vessels are mainly located in the perivascular interstitium adjacent to coronary artery and veins of the subepicardium. The typical perivascular distribution of lymphatics in the apical region of a normal fetal heart is shown in Figure 2. Lymphatics also show different morphologic features respect to blood vessels: the wall is thinner, the lumen is irregular and at time collapsed.

A similar pattern of expression of lymphatics and blood vessel markers is present in the adult heart (Fig 3). Interestingly, it appears that in the heart fluid drainage mainly occurs in the pericardial region, which exhibits high density of large size lymphatic vessels.

Adult Skin

Lymphatic vessels are also extensively present in the skin and are known to participate in a variety of physiological and pathological processes such as wound healing, inflammatory reaction, lymphoedema and scleroderma[727374]. Most of the lymphatic vessels have a patent lumen delineated by a tortuous and irregular profile. Some lymphatic vessels are completely or partially collapsed.

IHC analysis shows that human lymphatic vessels are consistently and intensely stained by Pdpn. Low intensity cross-reactivity was only found in some epithelial cells particularly in the basal layer of sebaceous glands. At variance with blood vessels, the endothelium and the subendothelial layer is negative for the vascular endothelial marker vWF. Blood vessels never show reactivity to Pdpn (Fig 4 A,B). Importantly, the specific

transcription factor for lymphatic commitment, Prox-1, is expressed in all endothelial cell nuclei lining lymphatic vessels (Fig 4 C,D).

CHARACTERIZATION OF LYMPHATIC VASCULATURE IN THE NORMAL RAT HEART

Immunohistochemistry

In agreement with previous observations made on the human heart, in the normal rat heart, lymphatic vessels are predominantly located in the subepicardium and in interstitial spaces surrounding arteries and veins (fig 5A,D,E). A small amount of thin lymphatic capillaries can be less frequently found between cardiomyocytes (Fig 5B). The quantitative estimation indicates that average lymphatic density is 2,66 ± 0.18 /mm^2, however the highest incidence of lymphatics was measured in the epimyocardium, where the density reaches values of 6,88 ± 0.53 /mm^2. Moreover, lymphatic vessels located in the latter region exhibit a larger luminal area compared with that found in vessels of the endo-and mid-myocardium. We did not observed lymphatic collectors surrounded by muscular layer in any of the hearts analysed in the present investigation (Fig 5D,E). The IHC analysis indicates that endothelial cells of lymphatics present in the normal rat heart express all the lymphatic markers LYVE-1, Pdpn and PROX-1 and none of them express the blood endothelial marker vWF (Fig 5A-E).

Ultrastructural and ImmunoGold detection of lymphatic vessels by TEM

TEM analysis of the normal rat heart allowed us to identify lymphatic vessels and to evaluate their specific ultrastructural features. Lymphatic vessels are often found in proximity of blood vessels and at time between cardiomyocytes (Fig 6A). The lymphatic wall is thinner with respect to blood vessels and capillaries. Basal lamina is

absent or at best discontinuous. In addition, interruption of the endothelial cell layer, due to the presence of fenestrations, is clearly documented (Fig 6 B).

ImmunoGold detection of LYVE1 expression revealed a specific presence of this protein in the cytoplasm and its extensions of lymphatics (Fig.6C). Furthermore, we observed that LYVE1 is not exclusively localized in transmembrane position (Fig 6C-D), but is also present in the extracellular space in proximity of transcytosis vesicles.

Fluorescence micro-lymphangiography on Whole Mount Preparations

Histological studies are usually restricted to bi-dimensional analysis, limiting the possibility to define the three-dimensional pattern of the microvascular network of the heart. In order to overcome this limitation, a whole mount micro-lymphangiography was performed on the rat skin and heart. After in vivo double labeling by infusion of fluorescent tracers (BSA-FITC and TRITC-dextran), whole rat ventricular wall samples were first subjected to a clearing procedure and then scanned by confocal microscope. This method allows to distinguish double-stained blood vessels (yellow fluorescence) from green fluorescent stained lymphatics that are only perfused by BSA-FITC. The imaging of whole mount thick samples of the skin clearly define the intricate network of blood and lymphatic vessels of this tissue (Fig 7A).

In the ventricular myocardium, images obtained by fluorescence micro-lymphangiography confirm the lymphatic location observed by the bi-dimensional approach. Most of BSA-FITC fluorescent lymphatic vessels run parallel to blood vessels, in the interstitium immediately adjacent to their wall (Fig 7B). Thin lymphatic capillaries can be found to a less extent between cardiomyocytes (Fig 7C).

CHARACTERIZATION OF LYMPHATIC VASCULATURE IN THE PATHOLOGIC RAT HEART

Myocardial infarction

To confirm the role of the lymphatic system in heart failure, as reported by Ishikawa et al.[37], in an experimental model we studied the effect of myocardial infarction on blood arterioles and on lymphatic vessels.

Seven days after coronary occlusion, in the acute remodeling phase, the number of SMA^{pos} arterioles in the infarct region results significantly increased. With the progression of scar maturation the number of arterioles slowly revert to normal values. Indeed, 21 days after induction of MI, when the lesion is replaced by mature scar tissue, arteriolar density is not significantly different with respect to normal myocardial (Fig 8B). At variance with these findings, lymphangiogenesis is not significantly activated one week after MI induction. The number of lymphatic vessels begin to rise in the infarct region during the last stage of scar formation, with a functionally relevant delay respect blood vessels (Fig 8C).

These results sustain the hypothesis that lymphatics are involved in fluids drainage and removal of inflammatory cells within necrotic tissues. Therefore, the lymphatic system, promoting scar maturation, play an essential role in the final assessment of myocardial remodeling after MI.

Genetically Determined and Pressure Overload Human Cardiac Hypertrophy

The histologic specimens of human HOCM myectomies stained with Masson's Trichrome exhibited well defined disease features such as myofiber disarray, and myocardial fibrosis. Hypertrophic and dismorphic cardiomyocytes appeared to be alternated with areas occupied by small size cells. Further analysis of fibrotic tissue showed different type of collagen accumulation. Widening of the interstitial space between myofibers and perivascular collagen accumulations were clearly detected in HOCM myocardium. In addition, a large band of fibrotic scar was present in the endocardium. An example of a low power microscopic field of a whole HOCM myectomy is documented in Figure 9A. Fibrous septa taking origin from the endocardial scar and extending to surround myocardial layers of hypertrophic cardiomyocytes were apparent. Thus, the collagen network in the HOCM heart is morphologically abnormal and increased in size compared with structurally normal hearts.

In the presence of such histomorphological pattern a strong rarefaction of vascular structures was expected, but only immunohistochemical detection of vWF positive capillaries showed a statistically relevant reduction in terms of density (number of vessel per mm^2 of analyzed tissue, Fig9C). The lymphatic behavior is totally different. The intricate myocardial remodeling observed in HOCM hearts was associated with a 20 fold increment of lymphatic vessel density in the fibrotic scar (data not shown) and a weaker but statistically significant 2,5 fold rise in the myocardium (Fig 9E).

In HOCM myectomies, immunohistochemical detection of ph-H3 showed high degrees of cell proliferation of all myocardial cell populations, including lymphatic endothelial cells, of which mitotic index reach 14% and 35% in myocardium and fibrotic scar

respectively (Fig 9F).

Hypertrophic heart specimens obtained from patients with aortic stenosis (AoS) were compared to HOCM. Similar increase in capillary and lymphatic vessels were found in term of density (Fig 9C-E). However, proliferative indexes of lymphatic endothelial cells were more than 20-fold higher in HOCM myocardium with respect to AoS. These observations suggest that genetically determined cardiac remodeling in HOCM patients is disease specific and characterized by active lymphangiogenesis.

DOXO induced cardiomyopathy

The mechanism of toxicity of DOXO is still unclear and there are no evidence about the direct involvement of angiogenesis and lymphangiogenesis. In experimental rats, treatment with DOXO for two weeks induces dilated cardiomyopathy, heart failure and death. The cardiomyopathy is characterized by multiple foci of inflammatory damage resulting in scattered focal deposition of collagen. The analysis of lymphatic structures conducted in this model of DOXO induced cardiomyopathy shows a 2-fold increase in vessel density (Fig 10A). Similar to the observations made in the MI model, lymphatic vessel density rises according to collagen deposition and for the establishment of myocardial fibrosis.

Therefore, in DOXO induced toxic insult on the heart, the lymphatic system also promotes replacement of the damaged myocardium by fibrotic tissues.

IM induced cardiomyopathy

As a consequence of three weeks of IM treatment, rats develop a pronounced cardiomyopathy. IM impairs cardiac function and produces a restrictive type of LV remodeling. Gross structural composition does not significantly change after IM treatment; the fractional volume of cardiac muscle is not heavily affected and no significant myocardial fibrosis is observed.

When the ratio of cardiac wet to dry weight is measured, compared to control values, an increase of "theoretical" water content in treated hearts is observed, especially with 100 mg/kg doses of IM (Fig 10C).

To evaluate the effect of IM on cardiac lymphatic system, the morphometric measurement of lymphatics was assessed by immunofluorescence. The quantitative estimation indicates that both 50 mg/kg and 100 mg/kg doses of IM induce a nearly 70% reduction of lymphatic vasculature (Fig 10B).

Ultrastructural detection and Immunogold staining of cardiac tissue by TEM indicate high levels of damage in lymphatic endothelial cells as a result of IM treatment. Significant alterations of subcellular structures were observed both in lymphatic and blood vessels of IM treated hearts. In lymphatic endothelial cells we detected specific marker of cellular stress, such the presence of swollen and degraded mitochondria and, occasionally, cytoplasmic accumulation of degradation products (Fig 10 D-E).

These data support the hypothesis that lymphatics are involved in normal fluids drainage and that the lack of their function may contribute to the development of IM related cardiomyopathy.

DISCUSSION

The importance of lymphatic system in the drainage of fluids and toxic metabolites in normal and pathological states of the organism is known, but studies of lymphatic vessels only lately became histological feasible, due to the recent discovery of several lymphatic endothelial cell-specific markers.

Even if little is known about the role and function of the lymphatic system in the heart, the recent identification of lymphatic endothelial cell-specific markers, the generation of transgenic "lymphatic-regulated" animal models and advanced lymphatic vascular imaging technologies led to a reevaluation of the importance of cardiac lymphatic vasculature in the control of heart function. A series of recent promising research studies have underlined the effect of active lymph drainage on heart function, especially in cardiac pathologies. Evidence that ischemic insults, like MI, can affect the lymphatic vasculature indicates its central role in the replacement of damaged myocardium by fibrotic tissue [37].

Significant information of our study is provided by the characterization of the lymphatic vasculature in mouse, rat, adult and fetal human samples. Notably, several methodologies, such as IHC, fluorescence micro-lymphangiography on whole mount preparations and TEM analysis were employed to elucidate the role of lymphatics.

The immunohistochemical analysis allowed us to define the lymphatic distribution in myocardial tissues. We consistently observed the location of large lymphatic vessels in the epicardial region of the heart, especially in the perivascular interstitium. On the other hand, lymphatic capillaries were mostly found in the myocardial parenchyma surrounding cardiomyocytes. On the contrary to that reported by the literature, we were not able to detect collecting lymphatic vessels surrounded by a small layer of smooth muscle cells. A possible explanation of this finding is that the

squeezing action produced by cardiomyocyte contraction during the cardiac cycle is sufficient to drain fluids and to pump out the lymph from internal lymphatic capillaries to collector ducts that are located in the extracardiac region.

The results of 2D analysis by IHC were confirmed by fluorescence micro-lymphangiography on whole mount preparations of the heart and skin. The 3D reconstruction of lymphatic and blood vasculature allowed us to observe the actual morphology and organization of both vascular systems in vivo. By this approach, lymphatic vessels were found to run parallel to blood ones, confirming the perivascular distribution documented by IHC. In addition, the typical tortuous aspect of lymphatics was clearly visible by the 3D confocal reconstruction of the vascular network in the skin. Thus, microlymphangiography can be easily applied to understand the pathophysiologic implication of cardiac lymphatics in heart failure.

Finally, TEM combined with Immunogold was used to detect the lymphatic vasculature and to analyze the ultrastructural features of lymphatic endothelial cells. In the normal heart, TEM identification of lymphatic vessels is facilitated by the evidence of typical sub-cellular features, such as fenestration and discontinuation of basal lamina, not easily detectable by other methodologies. In addition, Lyve-1 expression highlighted by Immunogold gave us further confidence about the real lymphatic nature of the observed vessel. Observations obtained in normal hearts by TEM confirmed the pattern of lymphatics distribution as shown by IHC and micro-lymphangiography. However in IM-induced cardiomyopathy, we observed ultrastructural damages on myocardial lymphatic endothelial cells. High incidence of swollen and degraded mitochondria and intense accumulation of degradation products in the cytoplasm of lymphatics were present.

In order to expand our knowledge and to elucidate the role of cardiac lymphatics, the lymphatic system in a mouse model of MI, in human myectomies of HOCM affected patients and in cardiomyopathies induced by drugs such as DOXO or IM were analyzed here.

Our observations confirm that the lymphatic system, promoting scar maturation, plays an essential role in the final assessment of myocardial remodeling after MI.

In HOCM patients the genetic defined cardiac remodeling observed in our study is disease specific and characterized by active lymphangiogenesis. Progressive septal tickening and collagen accumulation in HOCM myocardium is supported by a dense network of actively proliferating lymphatic vessels.

Further information earned by our study indicate that the integrity and density of lymphatic vessels in DOXO or IM induced cardiomyopathy are differently affected, confirming how these structures could be involved in the assessment of different pathologic states of the organ.

DOXO related cardiomyopathy was characterized by changes in lymphatics mimicking MI. In this specific cardiomyopathy, lymphatic vessels increase as a result of myocardial damage, in order to drain fluid and toxic metabolites from focal area of injury and to gradually favour the replacement of necrotic tissue by fibrosis.

At variance with these results, in IM related cardiomyopathy, myocardial lymphatic density is reduced and theoretical water content in treated hearts appears to be increased. Both these two phenomena may participate to the pathogenetic mechanism of cardiac dysfunction produced by IM and may be inversely related if the principal role of cardiac lymphatics in the drainage of fluids is considered.

Future perspectives

Our results suggest an active responsive role of lymphatic system in all the analyzed pathological condition, with the exception of IM induced cardiomyopathy. The observed tickening of lymphatic web has a "buffer effect" on myocardial microenvironment, improving dead cell clearance, waste material drainage and collagen deposition.

On the other hand, water content increase caused by the strong inhibitory effect of IM treatment on myocardial lymphangiogenesis could be a key event in the onset of IM induced cardiomyopathy. Myocardial edema is one of the typical feature of human myocarditis associated with diastolic dysfunction[75], conduction disturbances[76], microvascular compression[77] and tissue swelling.[78]

It has been clearly documented that c-Kit^{pos} Cardiac Progenitor cells (CPCs) play a central role in the control of cardiac homeostasis. Failure of CPC function may inevitably lead to a sequence of cellular events culminating in cardiac failure.

The direct effect of IM on CPCs through the inhibition of c-Kit receptor signaling was in part demonstrated by our preliminary studies on treated CPC growth. CPC ability to differentiate toward lymphatic phenotype was documented by the observation that a small fraction of freshly isolated CPCs cultured in standard conditions express the nuclear transcription factor Prox-1, a specific marker of lymphatic endothelial cells. Thus, an intrinsic commitment toward lymphatic differentiation was confirmed by the increased rate of Prox-1 expression after growing CPCs in MV2 conditioned medium. An additional supporting finding was the demonstration of a spontaneous tube formation on MATRIGEL^{TM} (BD, New Jersey, USA) by CPCs that was comparable with commercial human lymphatic cell line (HDLEC). To our knowledge, these data may open new ways for the understanding of

the origin of cardiac lymphatic system and its role in physiologic and pathological states of the heart.

Importantly, we show here that TK inhibition by IM exerts a negative effect on the ability of CPC to acquire a lymphatic phenotype in the presence of specific lymphangiogenic growth factors. Moreover, functional assays were able to document that IM hampered tube formation in vitro by CPCs comparable with the commercially available HDLEC cell line. A direct interference of TKI on PDGFR pathway is likely to be operative in the deleterious effects of IM on lymphatics. PDGF and its receptor system are fundamental for the regulation of angiogenesis including lymphangiogenesis. In agreement with this contention, however, when the incidence of PDGFRpos cells was measured in myocardial tissues, IM treated hearts had a lower content of this cell population (data not shown).

We advanced the hypothesis that CPCs may be involved not only in cardiomyogenesis and angiogenesis, but also in cardiac lymphangiogenesis.

The possibility of preventing cardiomyopathies by modulation of the lymphatic system may open new therapeutic options to unravel an unsolved clinical issue.

FIGURES AND LEGENDS

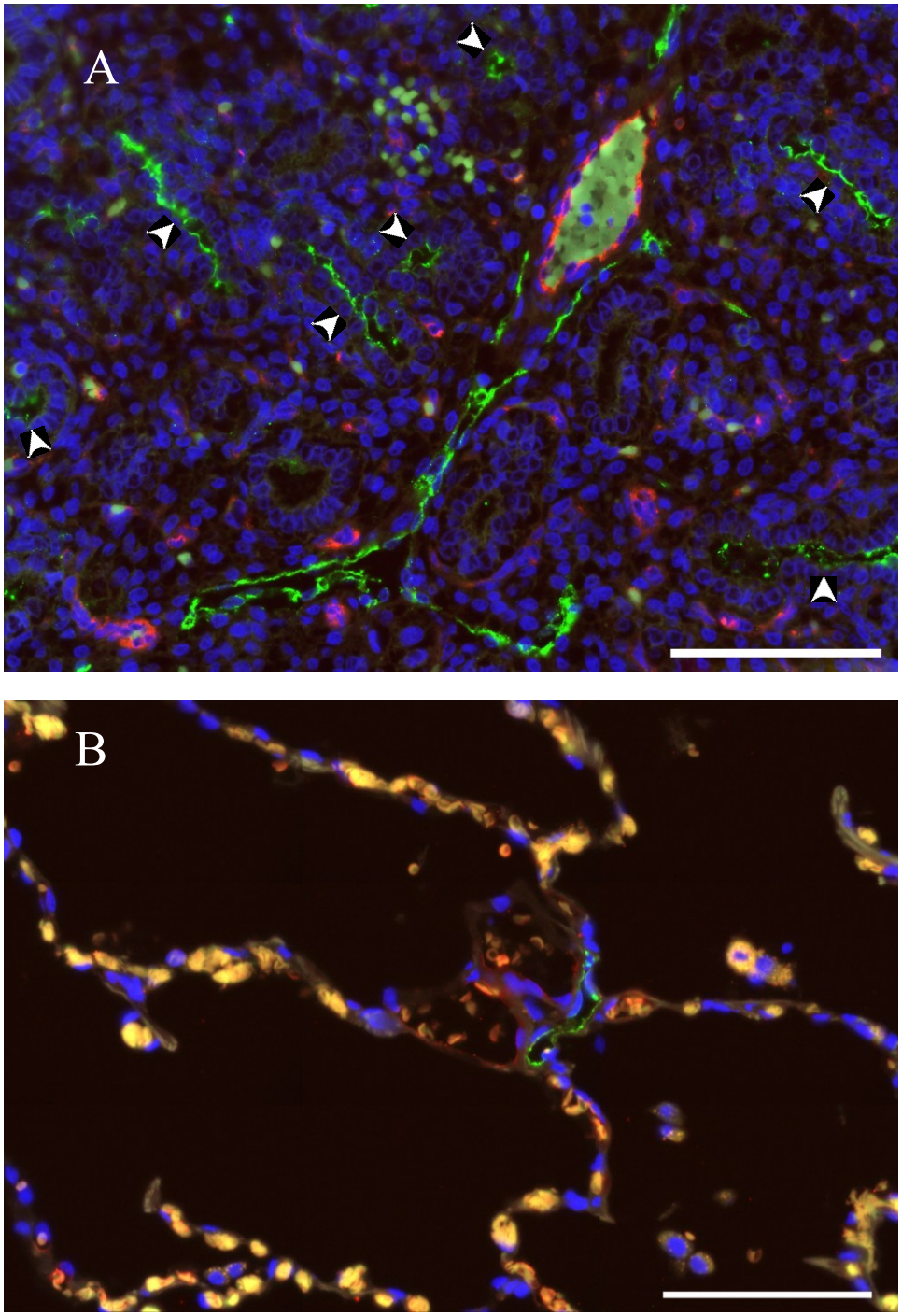

Figure 1. HUMAN LUNG. (A)Immunofluorescence image of a section of the human fetal lung in the canalicular phase of lung development stages. (B) Section of human adult lung showing small lymphatics in interalveolar areas. (A and B) Endothelial profiles are detected by the red fluorescence of vWF and lymphatic vessels by the green fluorescence for Pdpn antibody staining. Pdpn is also detected in the type I pneumocytes precursors in the terminal bronchiole (white arrowheads)

Scale bars 100 μM

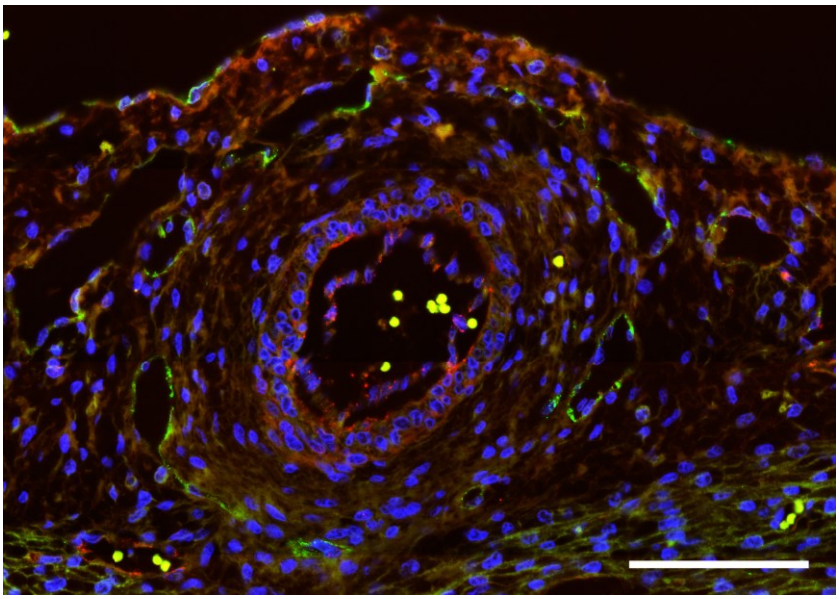

Figure 2. HUMAN FETAL HEART. Immunofluorescence image of the subepicardium in human fetal hearts. Pdpn expression (green fluorescence) is exclusively detected in lymphatic vessels typically located in perivascular spaces around coronary vessels whose lumen is identified by vWF expression (red fluorescence). Yellowish fluorescence corresponds to the autofluorescence of red blood cells that are present only in the lumen of blood vessels. Scale bar 100 μM

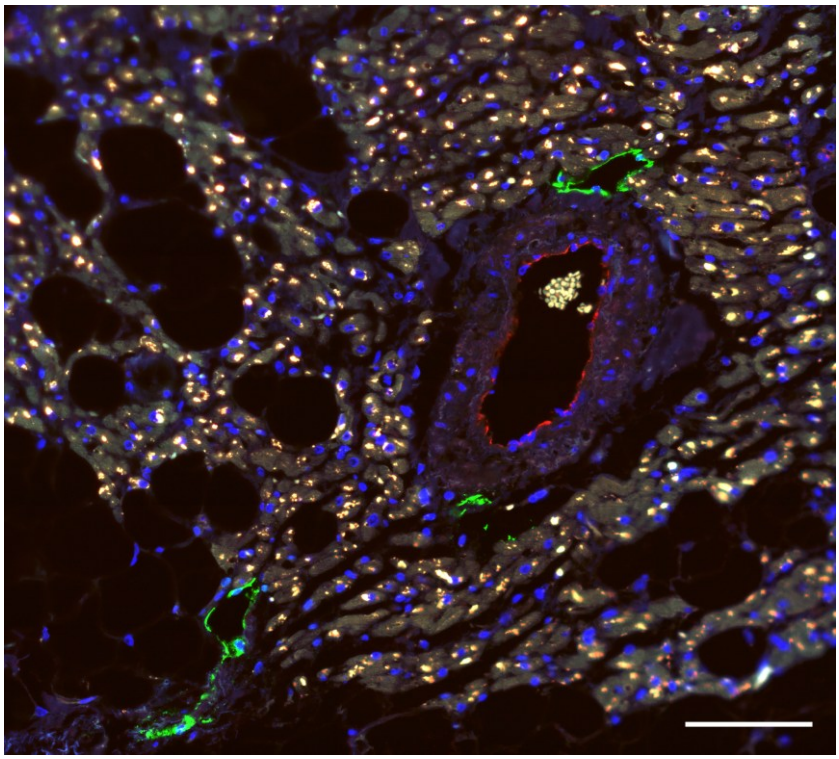

Figure 3. ADULT HUMAN HEART. Section of the epicardium of an adult human heart documenting by immunofluorescence the distinction between endothelial cells lining lymphatic vessels, labelled by Pdpn (green fluorescence) and those of a blood vessel (asterisk) labelled by vWF (red fluorescence). Red blood cells are recognized by autofluorescence in the lumen of the blood vessel. Large yellowish fluorescent spots correspond to phagocytic cells and small orange dots to lipofucsins. Scale bar 100 μM

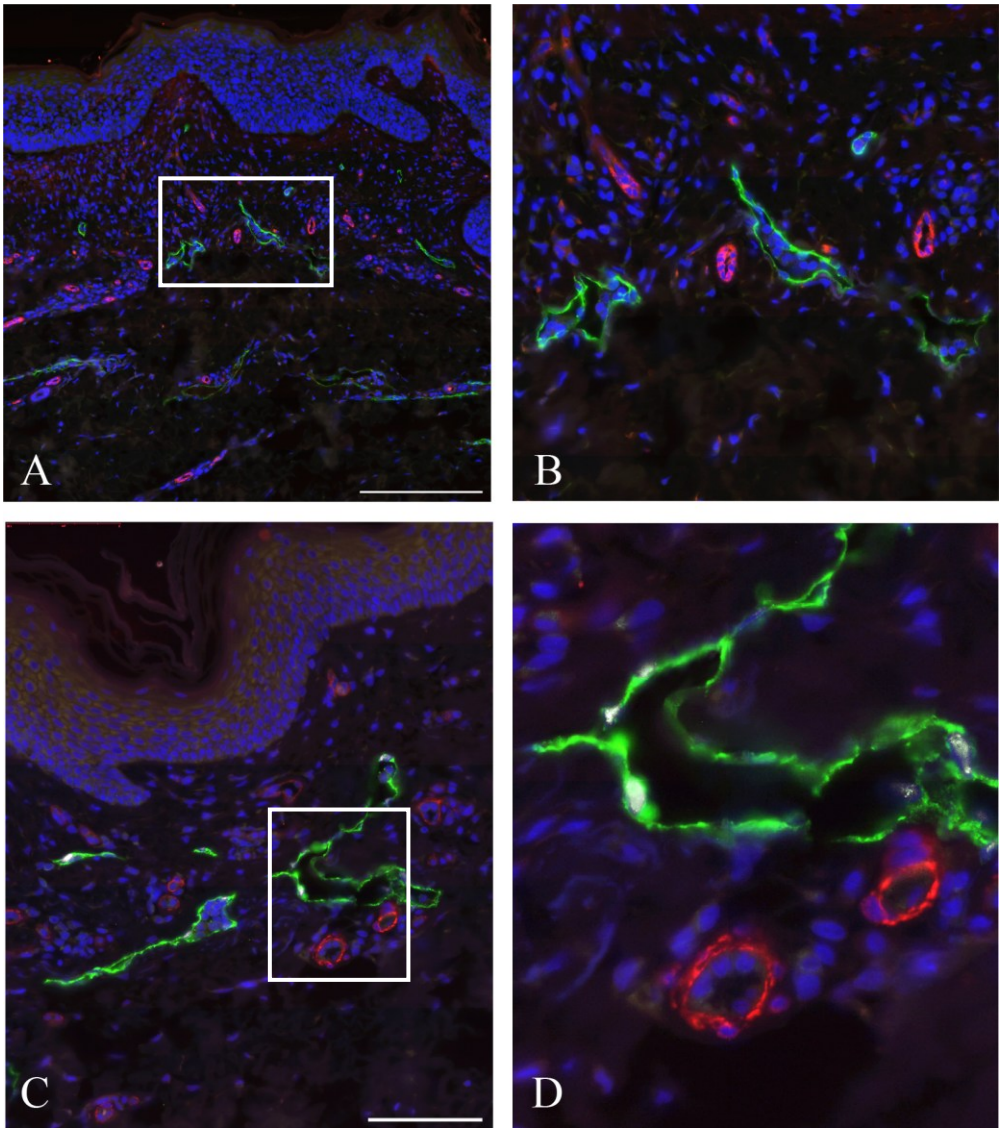

Figure 4. HUMAN SKIN. A-D: lymphatics are shown by the green fluorescence of Pdpn and blood vessels by vWF (red fluorescence) in the dermal aspect of the human skin. C-D: In association to pdpn, lymphatic endothelial cells nuclei express the specific transcription factor Prox-1 (white fluorescence). Microscopic images taken in B and D represent higher magnification of A and C, respectively, documenting the lack of double immunofluorescence in the same vessel. Scale bar A 250μM; C 100μM

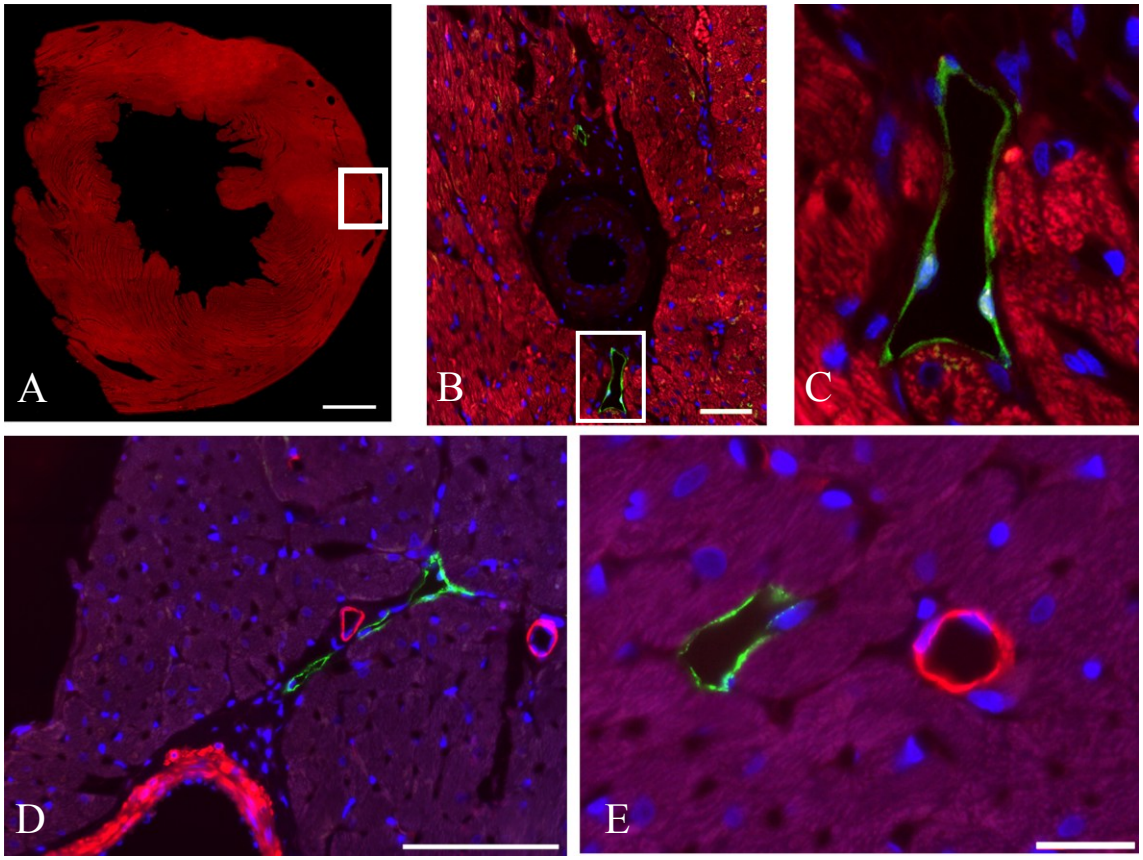

Figure 5. ADULT RAT HEART. A: low magnification of a cross section of the left ventricle (LV) of the rat heart as shown after immunofluorescence labelling of cardiomyocytes by a-sarcomeric actin (red fluorescence). Areas included in white rectangles are shown at higher magnifications in B and C, respectively, and document the typical distribution of lymphatic vessels labelled by Pdpn (green fluorescence) in the perivascular interstitium of the epicardium. The expression of the nuclear transcription factor Prox-1 (white fluorescence) by nuclei of lymphatic endothelial cells is better appreciable in C. D-E: lymphatics are shown by immunofluorescent labelling of the lymphatic marker Lyve-1 (green fluorescence) whereas arteries by a-smooth muscle actin (red fluorecence). Small lymphatic profiles can also lie in the interstitium between cardiomyocytes (E). Scale bar A 1mm; B 50 μM; D 100μM; E 25 μM

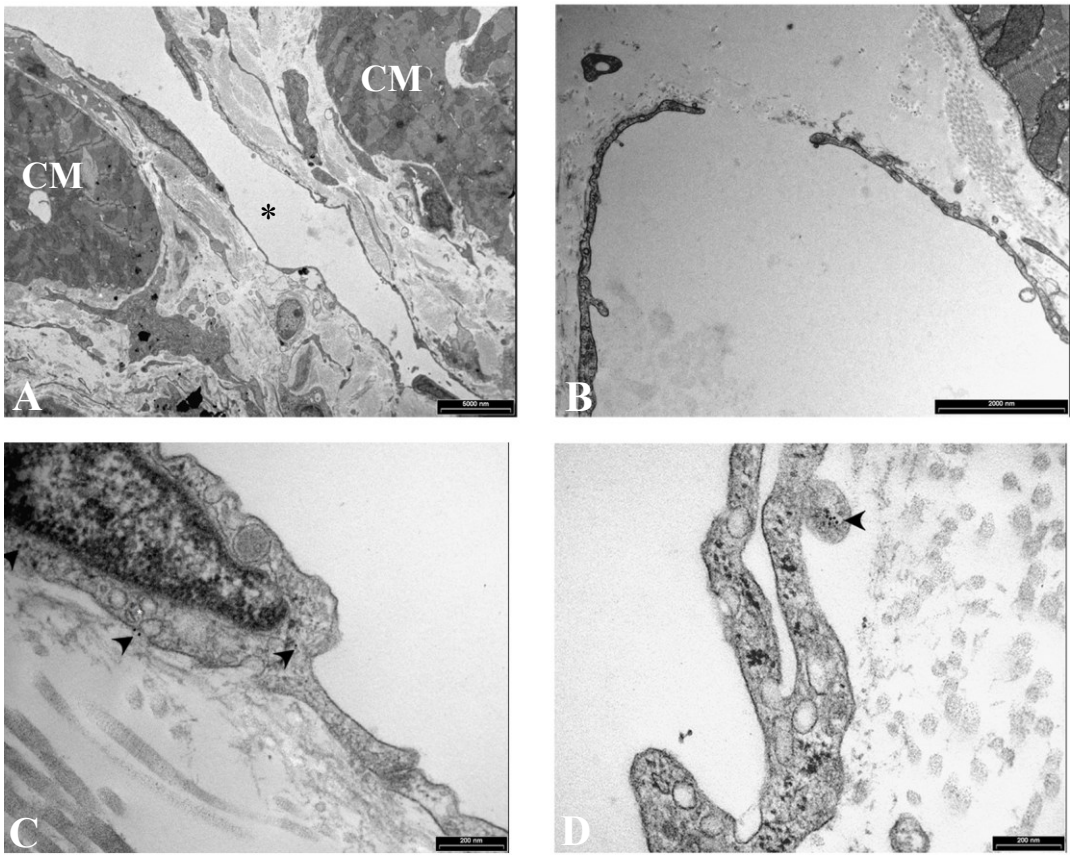

Figure 6. ULTRASTRUCTURAL AND IMMUNOGOLD DETECTION OF LYMPHATICS IN THE NORMAL RAT HEART. A: a lymphatic vessel located between cardiomyocytes (CM). A characteristic fenestrations of the endothelial cell layer is shown in figure B. C-D: immunogold using the specific lymphatic marker Lyve-1. Immunoreactivity for Lyve-1 is shown by small dark round dots (arrowheads) mostly located along the cytoplasmic extensions of lymphatic endothelial cells and in transmembrane position.

* lymphatic lumen

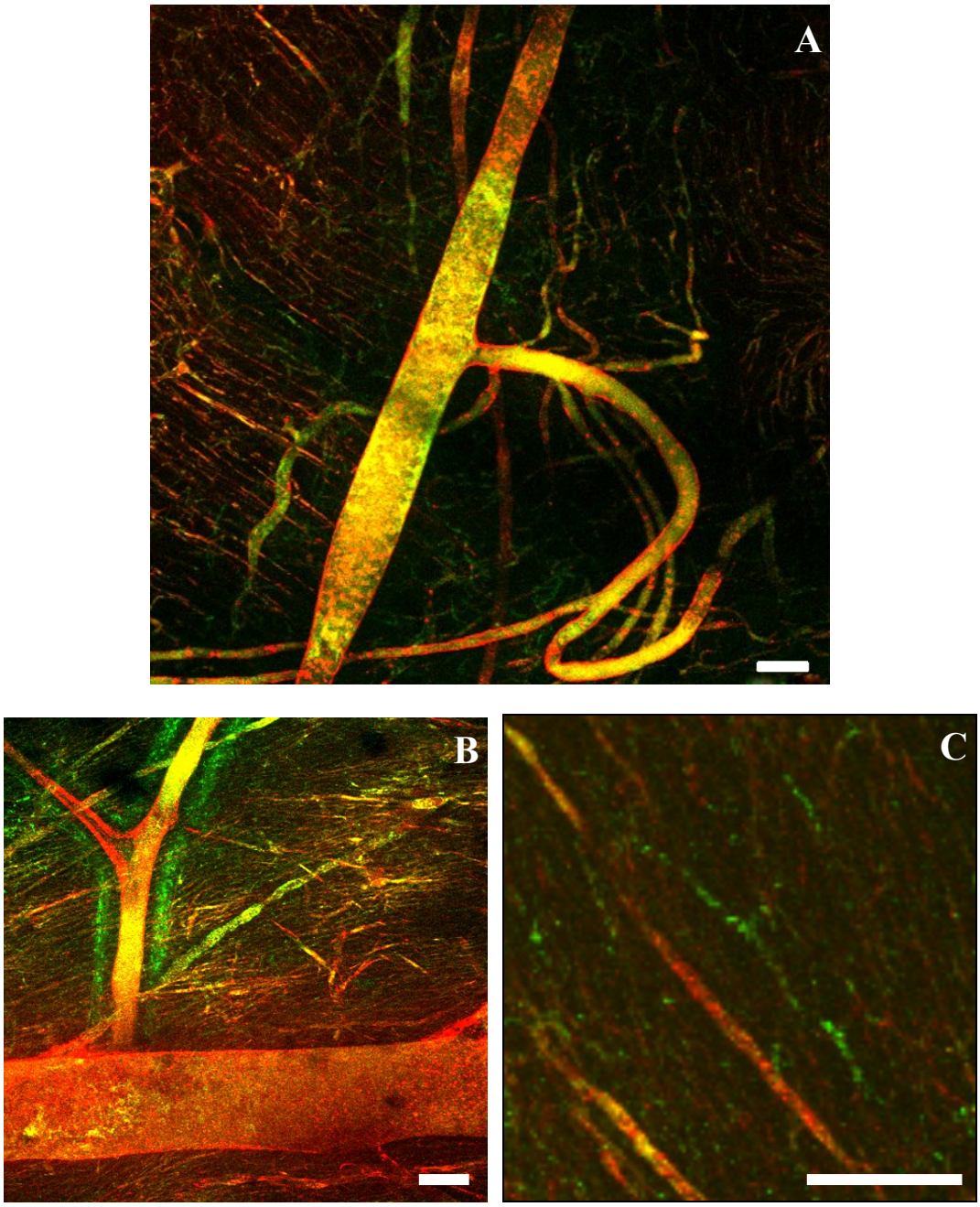

Figure 7. FLUORESCENCE MICRO-LYMPHANGIOGRAPHY ON WHOLE MOUNT PREPARATIONS OF THE RAT HEART AND SKIN. A: section of the rat skin showing by yellowish fluorescence a large (diameter approximately 100 mm) blood vessel and its branching as defined by the double fluorescence of FITC-BSA and TRITC-Dextran. Two lymphatics showing the typical irregular profile are recognized by the green fluorescence due to the selective perfusion by FITC-BSA. B and C: 3D reconstruction of the microcirculation in two sections of the left ventricle of an adult rat heart. Blood vessels (yellow fluorescence) show both injected dyes whereas lymphatics are perfused only by BSA-FITC tracer (green fluorescence). A large coronary vessel appears predominantly, although not uniquely, perfused by Dextran. Most larger lymphatics run parallel to blood vessels (B) and some lymphatic capillaries are detectable between cardiomyocytes (C). Scale bar : 100 μM

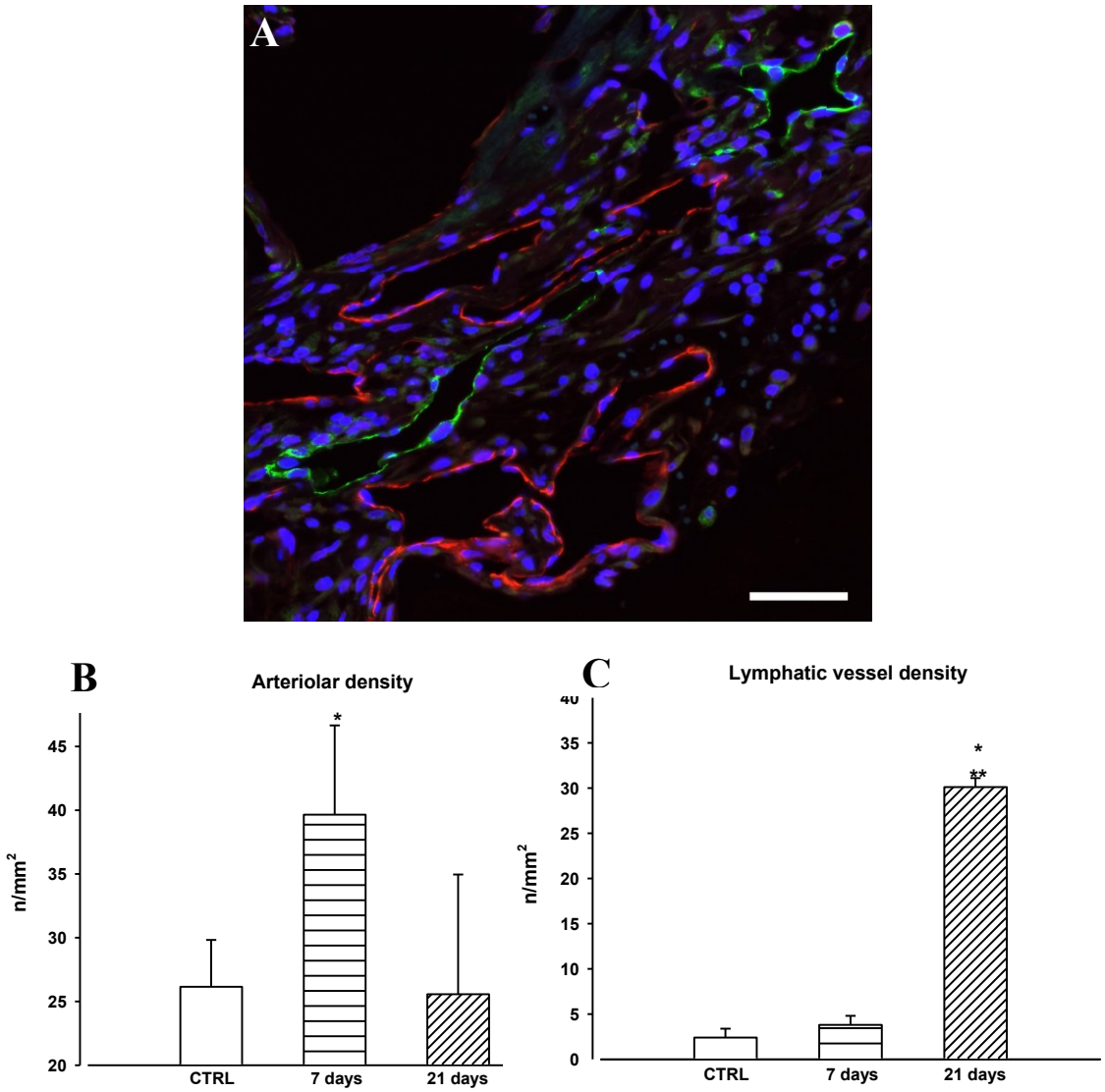

Figure 8. EFFECT OF MYOCARDIAL INFARCTION ON VASCULAR STRUCTURES. A: image of vascular components in the infarcted rat heart by immunofluorescence. Lymphatic vessels are detected by Lyve-1 (green fluorescence), whereas arterioles by specific anti α-SMA antibody (red fluorescence).B and C: bar graphs showing arteriolar and lymphatic density one week and 21 days after MI. Only arteriolar density significantly increases at 7 days, while lymphatic vessels are unchanged. After three weeks, corresponding to the completion of scar, lymphatic density results 6-fold higher than control while arteriolar density decrease to control (CTRL) values. Scale bar 50 μM

* $p<0.05$vs CTRL

** $p<0.05$vs 7 days

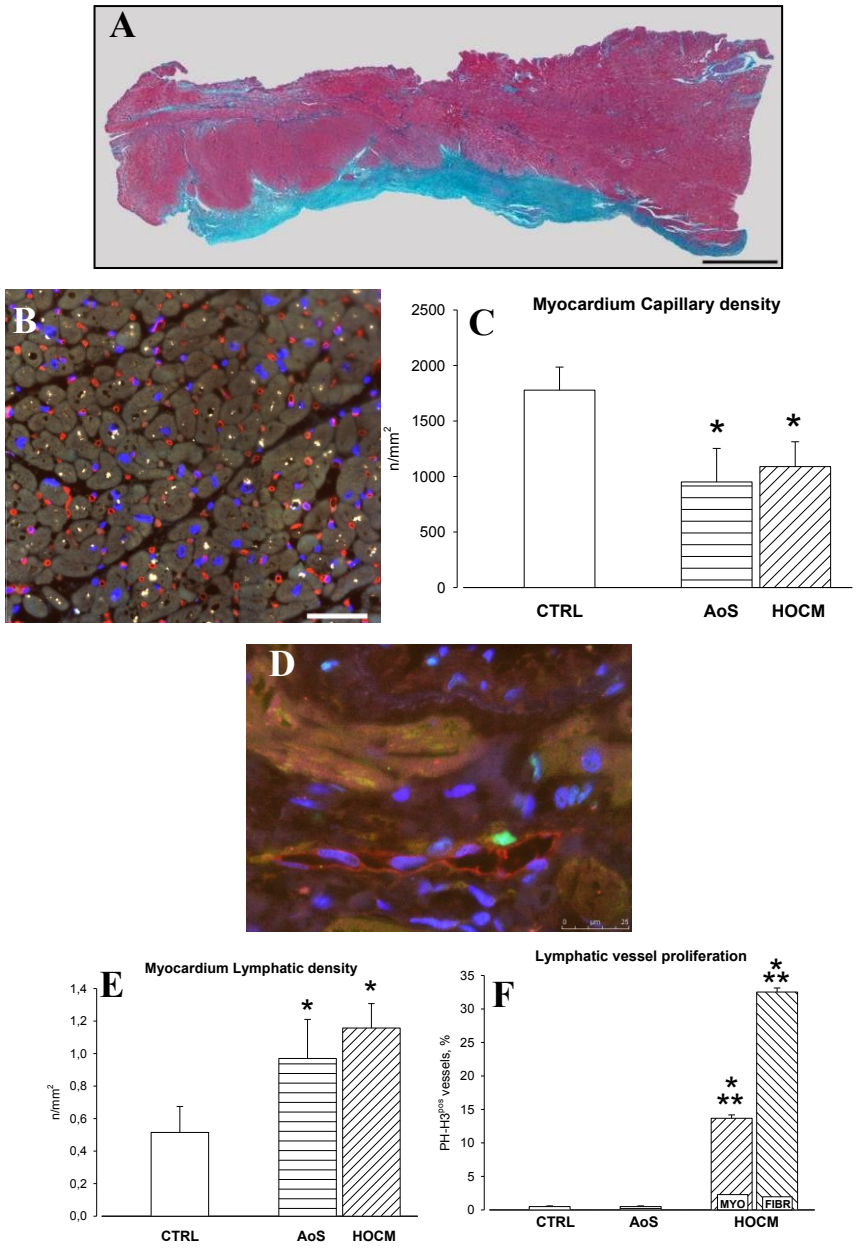

Figure 9. EFFECT OF HOCM VASCULAR STRUCTURES. A: Low power view of a section of the entire myectomy obtained from a HOCM patient and stained with Masson's Trichrome. The fibrotic tissue (bluish) involves a thick endocardial area from which collagen bundles seems to branch in interstitial septa separating myofibers (reddish). B and C: Immunohistochemical detection of vWF positive capillaries (red staining in B) showed a statistically relevant reduction in terms of density in both hypertrophic groups. D: Proliferating lymphatic vessels are detected by double staining of Pdpn (red fluorescence) and PhH3 (green fluorescence) E: Lymphatic vessel density showed a statistically significant 2,5 fold rise in the myocardium of HOCM and AoS. F: Mitotic Index of Cardiac lymphatics. In AoS the percentage of doubling lymphatic endothelial cells remain under 1% without significant differences respect control myocardium. In HOCM myectomies lymphatic mitotic index reach 14% and 35% in myocardium and fibrotic scar respectively. Scale Bars: B 50μm; D 25μm

* p<0.05vs CTRL; ** p<0.05vs AoS

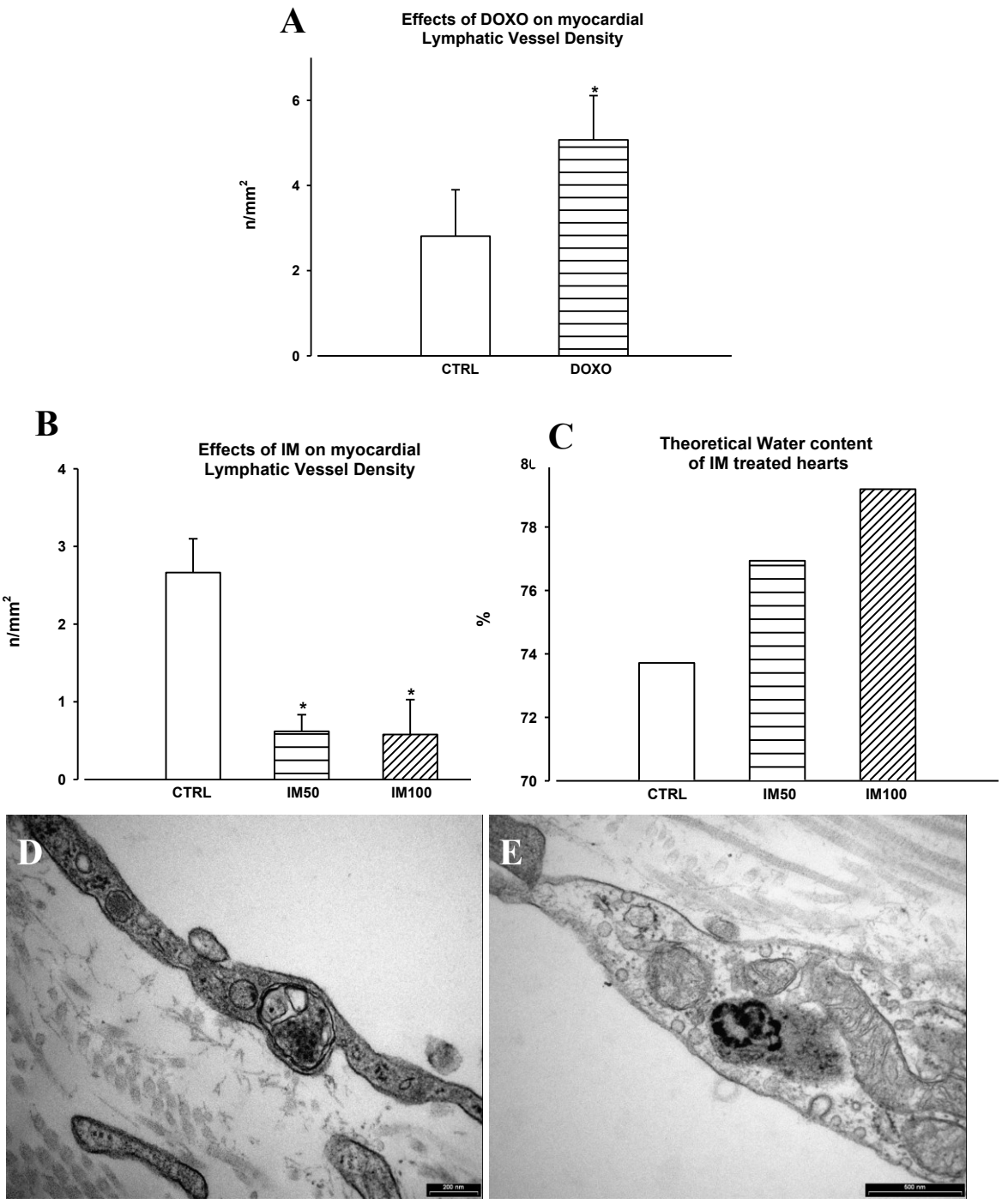

Figure 10. EFFECT OF DOXO AND IM TREATMENTS ON LYMPHATIC VESSELS OF THE RAT HEART. A: DOXO-induced cardiomyopathy is characterized by increased lymphatic density. B: IM- induced cardiomyopathic heart shows a significant reduction of lymphatic vessels coupled with an increased "theoretical" water content (C). D and E: TEM images documenting the presence of swollen and degrated mitochondria (D) and cytoplasmic accumulation of degradation products (E) in the lymphatic endothelial cells.

* $p<0.05$vs CTRL

REFERENCES

[1] Shayan, Ramin; Achen, Marc G.; Stacker, Steven A. "Lymphatic vessels in cancer metastasis: bridging the gaps". Carcinogenesis 1727:1729 2006
[2]"Definition of lymphatics". Webster's New World Medical Dictionary. MedicineNet.com.
[3] Cueni LN, Detmar M New insights into molecular control of the lymphatic vascular system and its role in disease. J Invest Dermatol 126: 2167-2177 2006
[4] Baluk P, Fuxe J, Hashizume H, Romano T, Lashnits E, Butz S, Vestweber D, Corada M, Molendini C, Dejana E, McDonald DM. Functionally specialized junctions between endothelial cells of lymphatic vessels. JEM 204: 2349-2362 2007
[5] Leak LV, Burke JF Fine structure of the lymphatic capillary and the adjoining connective tissue area. Am J Anat 118:785-809 1966
[6] Gerli R, Solito R, Weber E, Aglianó MSpecific adhesion molecules bind anchoring filaments and endothelial cell in human skin initial lymphatics. Lymphology 33: 148,157 2000
[7] Rossi A, Weber E, Sacchi G, Maestrini D, Di Cintio F, Gerli R.Mechanotransduction in lymphatic endothelial cells. Lymphology 40: 102-113 2007
[8] Bridenbaught EA, , Gashev AA, Zawieja DC. Lymphatic muscle: a review of contractile function. Lymphat Res Biol 1: 147-158 2003
[9] Witte, M.H., K. Jones, J. Wilting, M. Dictor, M. Selg, N. McHale, J.E. Gershenwald, and D.G. Jackson. 2006. Structure function relationships in the lymphatic system and implications for cancer biology. Cancer Metastasis Rev. 25:159–184.
[10] Ji, R.C. 2006. Lymphatic endothelial cells, tumor lymphangiogenesis and metastasis: New insights into intratumoral and peritumoral lymphatics. Cancer Metastasis Rev. 25:677–694]
[11] Tobler, N.E., and M. Detmar. 2006. Tumor and lymph node lymphangiogenesis–impact on cancer metastasis. J. Leukoc. Biol. 80:691–696.
[12] Sabin F on the origin of the lymphatic system from the veins and development of the lymph hearts and toracic duct in the pig. Am J Anat 1: 367-391 1902
[13] Huntington GS, McClure CFW The anatomy and development of the jugular lymph sac in the domestic cat (Felis domestica) Am J Anat 10: 177-311)(1910)
[14] Oliver G Lymphatic vasculature development. Nat Rev Immunol 4: 35-45(2004)
[15] Banerji S, Ni J, Wang SX, Clasper S, Su J, Tammi R, Jones M, Jackson DG LYVE-1, a new homologue of the CD44 glycoprotein, is a lymph-specific receptor for hyaluronan. J Cell Biol 144: 789-801 1999
[16] Jackson DG The lymphatic revisited: new perspectives from the hyaluronan receptor LYVE-1. Trends Cardiovasc Med 13: 1-7 2003
[17] Gale NW, Prevo R, Espinosa J, Ferguson DJ, Dominguez MG, Yancopoulos GD, Thurston G, Jackson DG Normal lymphatic development and function in mice deficient for lymphatic hyaluronan receptor LYVE-1. Mol Cell Biol 27: 595-504 2007
[18] Tammela T, Enholm B, Alitalo K, Paavonen K. The biology of vascular endothelial growth factors. Cardiovasc Res 65: 550-563 2005
[19] Tammela T, Zarkada G, Wallagard E, Murtomäki A, Suchting S, Wirzenius M, Waltari M, Hellström M, Schomber T, Peltonen R, Freitas C, Duarte A, Isoniemi H, Laakkonen P, Christofori G, Ylä-Herttuala S, Shibuya M, Pytowski B, Eichmann A, Betsholtz C, Alitalo K Blocking VEGF-R3 suppresses angiogenic sprouting and vascular network formation. Nature 454: 656-660 2008
[20] Kaipainen A, Korhonen J, Mustonen T, van Hinsbergh VW, Fang GH, Dumont D, Breitman M, Alitalo K. Expression of the fms-like tyrosine kinase 4 gene becomes restricted to lymphatic endothelium during development. Proc Natl Acad Sci USA 92: 3566-3570 1995
[21] Dumont DJ, Jussila L, Taipale J, Lymboussaki A, Mustonen T, Pajusola K, Breitman M, Alitalo K. Cardiovascular failure in mouse embryos deficient in VEGf receptor-3. Science 282: 946-949 1998
[22] Petrova TV, Mäkinen T, Mäkelä TP, Saarela J, Virtanen I, Ferrell RE, Finegold DN, Kerjaschki D, Ylä-Herttuala S, Alitalo K. Lymphatic endothelial reprogramming of vascular endothelial cells by the prox1 homeobox transcription factor. EMBO J 21: 4593-4599 2002
[23] Wigle JT, Harvey N, Detmar M, Lagutina I, Grosveld G, Gunn MD, Jackson DG, Oliver G. An essential role for Prox1 in the induction of the lymphatic endothelial cell phenotype. EMBO J 21: 1505-1513 2002)
[24] Wigle JT, Oliver G Prox1 function is required for the development of the murine lymphatic system Cell

98: 769-778 1999
[25] Hong YK, Harvey N, Noh YH, Schacht V, Hirakawa S, Detmar M, Oliver G. Prox1is a master control gene in the program specifying lymphatic endothelial cell fate. Dev Dyn 225: 351-357 2002
[26] Johnson NC, Dillard ME, Baluk P, McDonald DM, Harvey NL, Frase SL, Oliver G. Lymphatic endothelial cell identity is reversible and its mainteinance requires Prox1 activity. Genes Dev 22: 3282-3291 2008
[27] Schacht V, Ramirez MI, Hong YK, Hirakawa S, Feng D, Harvey N, Williams M, Dvorak AM, Dvorak HF, Oliver G, Detmar M. T1alpha/podoplanin deficiency disrupts normal lymphatic vasculature formation and causes lymphedema EMBO J 22: 3546-3556 2003
[28] Hirakawa S, Hong YK, Harvey N, Schacht V, Matsuda K, Libermann T, Detmar M Identification of vascular lineage-specific genes by transcriptional profiling of isolated blood vascular and lymphatic endothelial cells. Am J Pathol 162: 575-586 2003
[29] Albeda SM, Muller WA, Buck CA, Newman PJ Molecular and cellular properties of PECAM-1 (endoCAM/CD31): a novel vascular cell.cell achesion molecule. J Cell Bio 114:1059-1068 1991
[30] Young PE, Baumhueter S, Lasky LA . The sialomucin CD34 is expressed on hematopoietic cells and blood vessels during murine development. Blood 85:96-1051995
[31] Krieuber E, Breiteneder-Geleff S, Groeger M, Soleiman A, Schoppman SF, Stingl G, Kerjasschki D, Maured D Isolation and characterization of dermal lymphatic and blood endothelial cells reveal stable and functionally specialized cell lineages. J Exp Med 194:797-808 2001
[32] Allison PR, Sabison Jr DR, Experimental studies on the cardiac lymphatics Surg Forum 8: 271-271 1957
[33] Symbas Pn Cooper T, Gantner Jr GE, Willman VL, Lymphatic of the heart: anatomic effect following interruption of the drainage of the cardiac lymph Arch Path 81:573 1966
[34] Ludwig LL, Schertel ER, Pratt JW et al. Impairment of left ventricular function by acute cardiac lymphatic obstruction. Cardiovasc Res 33: 164-171 1997
[35] Patek PR The morphology of the lymphatics of the mammalian heart. Am J Anat 64: 203-234 1939
[36] Miller AJ, Pick R, Katz LN The importance of the lymphatics of the mammalian heart: experimental observations and some speculations. Circulation 29: 485-487 1964
[37] Cui Y Confocal imaging: blood and lymphatic capillaries. The scientific World Journal 6: 12-15 2006
[38] Zawieja DC, Davis KL, Schuster R, Hinds WM, Granger HJ. Distribution, propagation and coordination of contractile activity in lymphatics. Am J Physiol 264: H1283-H1291
[39] Mislin H. Experimental detection of autochthonous automatism of lymph vessels. Experientia 17: 29-30 1961
[40] Y. Ishikawa, Y Akishima-Fukasawa, K Ito, Y Akasaka, M Tanaka, R Shimokawa, M Kimura-Matsumoto, H Morita, S Sato, I Kamata, T Ishii Lymphangiogenesis in myocardial remodelling after infarction. Histopathology 51: 345-353 2007
[41] Williams LT "Signal transduction by the platelet-derived growth factor receptor". Science 243:1564–1570 1989
[42] Heldin CH, Westermark "Platelet-derived growth factor: three isoforms and two receptor types". Trends Genet. 5:108–11 1989
[43] Hellstrom M, Kalen M, Lindahl P, Abramsson A, Betsholtz C. Roleog PDGF-B and PDGFR-b in recruitment of vascular smooth muscle cells and perycites during embryonic blood vessel formation in the mouse. Development 126: 3047-3055 1999
[44] Gerhart H, Golding M, Fruttiger M, Ruhrberg C, Lundkvist A, Abramsson A, Jeltsch M, Mitchell C, Alitalo K, Shima D et al, VEGF guides angiogenic sprouting utilizing endothelial tip cell filopodia. J. Cell Biol 161:1163-1177 2003
[45] Cao R, Brakenhielm E, Pawliuk R, Wariaro D, Post MJ, Wahlberg E, Leboulch P, Cao Y, Li X, Pietras K, Widenfalk J, Ostman A, Eriksson U. Angiogenic synergism, vascular stability and improvement of hind-limb ischemia by a combination of PDGF-BB and FGF-2. Nat Med; 9:604-13 2003
[46] Cao R, Bjorndahl MA, Religa P, et al. PDGF-BB induces intratumoral lymphangiogenesis and promotes lymphatic metastasis. Cancer Cell; 6:333-45 2004
[47] Semsarian C, Seidman CE. Molecular medicine in the 21st century. Intern Med J. 2001 Jan-Feb;31(1):53-9.
[48] Maron BJ, Bonow RO, Cannon RO III, Leon MB, Epstein SE. Hypertrophic cardiomyopathy:

interrelation of clinical manifestations, pathophysiology, and therapy. N Engl J Med, 316: 844-852; 1987.
[49] Wigle ED, Sasson Z, Henderson MA, Ruddy TD, Fulop J, Rakowski H, Williams WG. Hypertrophic cardiomyopathy: the importance of the site and extent of hypertrophy: a review. Prog Cardiovasc Dis,28: 1-83; 1985.
[50] Braunwald E, Lambrew CT, Rockoff SD, Ross J, Morrow AG. Idiopathic hypertrophic subaortic stenosis, I: a description of the disease based upon an analysis of 64 patients. Circulation, suppl 4: 3-119; 1964.
[51] Maron BJ, Nichols PF, Pickle LW, Wesley YE, Mulvihill JJ. Patterns of inheritance in hypertrophic cardiomyopathy: assessment of M-mode and two-dimensional echocardiography. Am J Cardiol, 53: 1087-1094; 1984.
[52] Maron BJ, Gottdiener JS, Epstein SE. Patterns and significance of distribution of left ventricular hypertrophy in hypertrophic cardiomyopathy: a wide-angle, two-dimensional echocardiographic study of 125 patients. Am J Cardiol, 48: 418-428; 1981.
[53] Watkins H, Rosenzweig A, Hwang D-S, Levi T, McKenna WJ, Seidman CE, Seidman JG. Characteristics and prognostic implications of myosin missense mutations in familial hypertrophic cardiomyopathy. N Engl J Med., 326: 1108-1114; 1992.
[54] Roberts CS, Roberts WC. Morphologic features. In: Zipes DP, Rowlands DJ, eds. Progress in Cardiology 2/2. Philadelphia, Pa: Lea & Febiger; 1989:3-22.
[55] Ciró E, Nichols PF, Maron BJ. Heterogeneous morphologic expression of genetically transmitted hypertrophic cardiomyopathy: two-dimensional echocardiographic analysis. Circulation, 67: 1227-1233; 1983.
[56] Hecht GM, Klues HG, Roberts WC, Maron BJ. Coexistence of sudden cardiac death and end-stage heart failure in familial hypertrophic cardiomyopathy. J Am Coll Cardiol, 22: 489-497; 1993.
[57] Teare D. Asymmetrical hypertrophy of the heart in young patients. Br Heart J, 20: 1-18; 1958.
[58]Doolan et al.Hypertrophic cardiomyopathy: from “heart tumour” to a complex molecular genetic disorder. Heart Lung and Circulation; 13: 15–25, 2004.
[59] Maron BJ. Hypertrophic cardiomyopathy. Lancet; 350: 127-133, 1997.
[60] Krause DS, Van Etten, RA Tyrosine kinases as targets for cancer therapy. N. Engl. J. Med. 353, 172–187, 2005
[61] Tilly, H., Lepage, E., Coiffier, B., Blanc, M., Herbrecht, R., Bosly, A., Attal, M., Fillet, G., Guettier, C., Molina, T.J., Gisselbrecht, C., Reyes, F. Intensive conventional chemotherapy (ACVBP regimen) compared with standard CHOP for poor-prognosis aggressive non-Hodgkin lymphoma Blood, 102, 4284 2003
[62] Jones, S.E.; Savin, M.A.; Holmes, F.A. J. Clin. Oncol., 24, 538, 2006
[63] Branca, M. A. Multi-kinase inhibitors create buzz at ASCO. Nature Biotech. 23, 639, 2005
[64] Kerkela R.; Grazette L.; Yacobi R.; Iliescu C.; Patten R.; Beahm C.; Walters B.; Shevtsov S.; Pesant S.; Clubb FJ.; Rosenzweig A.; Salomon RN.; Van Etten RA.; Alroy J, Durand JB.; Force T. Cardiotoxicity of the cancer therapeutic agent imatinib mesylate. Nat Med, , 12, 908-916 2006
[65] Force T.; Krause DS.; Van Etten RA. Molecular mechanisms of cardiotoxicity of tyrosine kinase inhibition, Nature medicine 7, 332-44, 2007
[66] Deininger, M., Buchdunger, E. & Druker, B. J. The development of imatinib as a therapeutic agent for chronic myeloid leukemia. Blood 105, 2640–2653, 2005
[67] Giles FJ, O’D’wyer M, Swords R Class effects of tyrosine kinase inhibitors, Leukemia, 2009
[68] Lauweryns JM (1971) The blood and lymphatic microcirculation of the lung. Pathol Annu 6:365–415.
[69] Nagaishi C (1972) Chapter III: Lymphatic system. In Functional Anatomy and Histology of the Lung. Baltimore, MD, University Park Press, 102–179.
[70] Okada Y, Ito M, Nagaishi Ch (1979) Anatomical study of the pulmonary lymphatics. Lymphology 12:118–124.
[71] Leak LV (1980) Lymphatic removal of fluids and particles in the mammalian lung. Environ Health Perspect 35:55–76.
[72] Cueni LN, Detmar M. New insights into the molecular control of the lymphatic vascular system and its role in disease. J Invest Dermatol;126:2167-77 2006
[73] Jackowski S, Janusch M, Fiedler E, et al. Radiogenic lymphangiogenesis in the skin. Am J Pathol; 171:338-48 2007

[74] Kajiya K, Kunstfeld R, Detmar M, Chung JH. Reduction of lymphatic vessels in photodamaged human skin. J Dermatol Sci;47:241-3 2007
[75] Pogatsa G, Dubecz E, Gabor G: The role of myocardial edema in the left ventricular diastolic stiffness. Basis Res Cardiol 1976, 71:263-269.
[76] Morimoto S, Kato S, Hiramitsu S, Uemura A, Ohtsuki M, Kato Y, Sugiura A, Miyagishima K, Yoshida Y, Hishida H: Role of myocardial interstitial edema in conduction disturbances in acute myocarditis. Heart Vessels 2006, 21:356-360
[77] Manciet LH, Poole DC, McDonagh PF, Copeland JG, Mathieu-Costello O: Microvascular compression during myocardial ischemia: mechanistic basis for no-reflow phenomenon. Am J Physiol 1994, 266:H1541-50.
[78] Oka K, Oohira K, Yatabe Y, Tanaka T, Kurano K, Kosugi R, Murata M, Hakozaki H, Nishikawa T, Tsutsumi Y: Fulminant myocarditis demonstrating uncommon morphology-a report of two autopsy cases. Virchows Arch 2005, 446::259-264.